PHYSICOCHEMICAL INTERACTIONS OF SOURCE-ROCKS WITH INJECTED WATER-BASED FLUIDS

A Thesis

by

ZAID R. ABDULSATTAR

Submitted to the Office of Graduate and Professional Studies of
Texas A&M University
in partial fulfillment of the requirements for the degree of

MASTER OF SCIENCE

Chair of Committee,	Robert H. Lane
Co-Chair of Committee,	Berna Hascakir
Committee Member,	Yuefeng Sun
Head of Department,	A. Dan Hill

May 2015

Major Subject: Petroleum Engineering

Copyright 2015 Zaid R. Abdulsattar

ABSTRACT

Water-based fracturing fluids contain polymers to function either as fluid viscosifiers or friction-reduction agents. Whereas much work has been done on optimizing these functions, little or no published work focuses on their chemical interactions with the rock they are targeting. Co-polymers of polyacrylamide are used in slick-water fracturing, while Guar gum or one of its derivatives is used as a base for linear or cross-linked gels. This thesis reports studies on the adsorption behavior of some, primarily, guar-based polymers onto the surface of source rock outcrop samples in order to provide a better picture of the interactions of polymers with these rocks. Outcrop samples from the Barnett, Eagle Ford, and Marcellus were collected, analyzed for mineralogy and total organic carbon, and then exposed to different polymer solutions under elevated temperature and moderately elevated pressure. Viscosities of these polymer solutions were measured before and after exposing them to the rock in order to establish a correlation between polymer adsorption and the rock mineralogy and organic content. Results indicate that there is a significant correlation between the adsorption behavior of the polymer and the rock mineralogy and its organic carbon. Polymer adsorption is in agreement with cation exchange mechanisms as described in earlier work. Cationic polymers are more prone to be adsorbed on the surface of the rock than non-ionic polymers. The importance of polymer adsorption has not yet been determined. It is speculated that due to viscosity reduction resulting from polymer adsorption, wellbore clean-up could be enhanced through the use of this property. It could also have detrimental impacts on hydrocarbon

production. This work also shows that oxidizing breakers might be spent on removing the organic content of the rock rather than being spent on breaking cross-linked gels, especially in rocks with high organic content. The results from this work point out that fluid-rock interactions are significant, and that further research regarding source-rock polymer interactions and its effects on hydrocarbon production is needed.

DEDICATION

This thesis is dedicated to my parents, friends, and all those who helped me through thick and thin for the past 26 ½ years.

This thesis is also dedicated to my dog Luke, whose loving memory will always be beside me.

This thesis is also dedicated to my dog Slash, who is a good boy.

ACKNOWLEDGEMENTS

I would like to express my sincere gratitude to both my advisers, Dr. Robert Lane and Dr. Berna Hascakir. Without their constant support, endless revisions of this document, and direction to use specific scientific tools, this work would not have existed.

Special thanks are also given to members of the Crisman Institute, whom without their generous funding, this project would not have existed.

I would also like to thank Dr. Yuefeng Sun for being my committee member.

I would like to thank the faculty and staff in the department of petroleum engineering. Without their support and encouragement, my work would have been many, many times harder.

I would like to thank members of the Heavy Oil, Oil Shales, Oil Sands, and Carbonate Analysis Recovery Methods (HOCAM) for their help in conducting the thermos-gravimetric and FTIR measurements.

Finally, I would like to thank Ellington Laboratories for conducting the mineralogy testing.

NOMENCLATURE

FTIR	Fourier Transform Infrared Spectroscopy
CEC	Cation Exchange Capacity
XRD	X-ray Diffraction
TGA	Thermogravimetric Analysis
cP	Centipoise
meq	Milliequivalent
KCl	Potassium Chloride
NaCl	Sodium Chloride
$MgCl_2$	Magnesium Chloride
TOC	Total Organic Content
G/M Ratio	Galactose to Mannose ratio
wt%	Weight Percent
M	Thousand
MM	Million
CMC	Carboxymethyl Cellulose
CAS	Chemical Abstract Number
Bbls	Barrels

TABLE OF CONTENTS

Page

LIST OF FIGURES

Page

LIST OF TABLES

Page

1. INTRODUCTION AND LITERATURE REVIEW*

1.1 Introduction

The ever-increasing demand for energy has prompted oil and gas operators and service companies to develop technology that can sustain the current shale boom. Shale gas production is projected to increase by two fold by 2040 as a result of such increase in demand (Miller, 2013).

Shale is an often incorrectly used term. The terms "shale" and "source rock" are commonly used interchangeably in the oil and gas industry to refer to formations where hydrocarbons were generated and are currently produced. By definition, source rocks are considered shales if the clay content is greater than 50%. (Merriman et al., 2003). Some shales are indeed source rocks, but not all source rocks are shales because they do not actually contain enough clay content to merit the naming "shale."

1.2 Overview of Hydraulic Fracturing

Hydrocarbons from source rock plays cannot be commercially produced without some form of stimulation due to the ultra-low permeability of these reservoirs. A stimulation method that is currently being used in numerous source rock plays is multistage hydraulic fracturing of horizontal wellbores. This technology involves pumping water-based fluids

---

* Part of this thesis is reprinted with permission from "Physico-chemical Interaction of Source-rocks with Injected Water Based Fluids" by Abdulsattar, Z., Agim, K., Lane, R., et al. Paper SPE 173727 presented at the SPE International Symposium on Oilfield Chemistry in the Woodland, Texas, U.S.A., 14-16 April. Copyright 2015 by the Society of Petroleum Engineers.

and varying amounts of sand into the formation above parting pressure in order to create and prop fractures in the rocks.

These fractures provide pathways for the hydrocarbons to flow from the reservoir into the wellbore. The sand is a propping agent to help keep the fractures open after the stimulation procedure is completed. Hydraulic fracturing in source rocks differs from that in sandstone formations because source rocks cannot be commercially produced without stimulation. Therefore hydraulic fracturing is very essential to the shale oil and gas industry.

As the industry moved toward utilizing source rocks as a source of hydrocarbons in the last two decades, several methods were developed to hydraulically fracture those formations. However, while numerous studies were done to optimize fracture fluids formulations, the industry lagged in its understanding of the interactions of source rocks with such hydraulic fracturing fluids. Source rocks usually contain relatively large amounts of clays, many of which could react with the fracturing fluids, and the results of such reactions must be characterized to design more suitable fracturing fluids for such reservoirss. Also, the fate of the organic additives in fracturing fluids after contacting source rock formations must be properly understood for reasons such as understanding damage mechanisms and the potential for flow-back water reuse.

1.3 Overview of Hydraulic Fracturing Fluids

The process of hydraulic fracturing was first carried out in sandstone formations in 1947 (Montegomery, 2010). Water was first used as a base for fracturing fluids in 1953 (US

Patent 3058909) (Kern, 1962). Then a water solution of guar gum was cross-linked by borate salts for Arco in 1962 (Montgomery and Smith, 2010). Hydraulic fracturing fluid technology has evolved over time from gelled napalm, crude oil and gasoline to cross-linked and slick-water fluids.

Cross-linked polymers such as guar gum are used as a gelling agent to obtain a fluid that is viscous enough to carry large amounts of proppant (Montgomery, 2013). When guar gum is mixed with water without cross linker, the result is a viscous fluid often referred to as a linear gel (Montgomery, 2013). The linear gel is capable of achieving viscosities on the order of 100s of centipoises, which limits its proppant carrying capacity. A cross linker such as borate salt is used to alleviate this problem (Montgomery, 2013). The result is a three-dimensionally structured gel that has a much higher effective viscosity than can be attained with linear gels.

After the hydraulic fracturing stimulation is complete, and in order for the well to start producing, it has to undergo a period called "wellbore clean-up" when the fracturing fluid pumped must be broken into a lower viscosity fluid, which facilitates the flow-back of the residual polymer to the surface (Montgomery, 2013). Oxidizing breakers such as ammonium disulfate and sodium bromate are commonly used to reduce the viscosity of the fracturing fluid and help with the clean-up process (Montgomery, 2013).

Hydraulic fracturing was first introduced into source rock formations, specifically Barnett Shale in mid 1980s. Early treatments used cross-linked gels then gradually switched to slick-water treatments due to their perceived improvements in wellbore clean-

up and lower costs (Leonard et al., 2007). However, crosslinked gels are still used nowadays in many source rock plays.

Slick-water fluid is water that has been slickened with a friction reducer or a low concentration linear gel. The purpose of this "slickening" is to reduce the friction of the fluid with the pipe as it travels down. This reduces the pressure drop across the pipe, allowing for higher pumping rates (Palisch, 2010). An analysis of some 293 wells in the Barnett Shale concluded that slick-water generally outperformed cross-linked fluids in terms of hydrocarbon production rates (Greiser et al., 2008). It was generally believed that using slick-water fluids provided better proppant conductivity because it causes less formation damage than high viscosity fluids. High viscosity fluids such as crosslinked gels can incompletely break and leave behind quantities of polymers in the sand particles keeping the fractures open (proppant pack), causing a reduction in production rates (Kostenuk and Browne, 2010). That reduction in permeability is a result of an impairement to the proppant pack conductivity. Proppant pack conductivity is the ability of the propping medium to function as a conduit to transmit fluids (Weaver et al., 2007). Any damage to this medium can have a detrimental impact on the proppant conductivity.

1.4 Damage Mechanisms Caused by Hydraulic Fracturing Fluids

Several damage mechanisms to the proppant pack conductivity have been proposed and proven over the years. Fines migration was described by (Palisch et al., 2007) as how the proppant might crush and plug the pores in the proppant pack. Proppant embedment is another mechanism where proppants might embed into the soft source rock formation,

reducing the fracture conductivity (Alramahi and Sundberg, 2012). Proppant diagenesis is another proposed damage mechanism where the high temperature of the reservoir coupled with high stress causes dissolution and precipitation, causing a reduction in the proppant porosity (Weaver, 2005). Another damage mechanism that has been described is the plugging of the proppant pack due to poor polymer breaking (**Fig. 1**). Unbroken fracturing fluid (polymer) can cause impairment in the proppant pack permeability, which could reduce hydrocarbon production rates (Hawkins, 1988). Proppant pack permeability reduction was observed even at low polymer concentrations.

Fig. 1: Unbroken polymer gel residue can plug the proppant pack

It is not always easy to study the extent of formation damage that could occur as a result of fracturing fluids and all their components mixed together. Therefore, it is

necessary to study the impact of each component first, then move on using combinations of additives.

1.5 Clay-Polymer Interactions

Source rocks are known to have varying degrees of clay content ranging from 10% in the Eagle Ford shale to 50% or more in the Barnett. Studies of shale-drilling fluid interactions have been fairly prevalent in the oil and gas industry because of the problems those shales cause while drilling (Remvik, 1995). For decades, drilling in shale formations has increased drilling time, and often has caused borehole instability problems, mainly due to the clay's sensitivity to water-based fluids (He et al., 2014). Studies were done to characterize the impact of shale destabilization on wellbore instability (Mody and Hale, 1993; Ewy and Morton, 2009), while others studied drilling fluid imbibition into shale formations (Ewy and Stankovich, 2002; Remvik, 1995).

Clay polymer interactions have been described as early as 1874 when Schloesing (1874) was prompted by the biostability of soil organic matter when exposed to polymers. Polymer adsorption is one mechanism of interaction, where the polymer is adsorbed onto the surface of clays, due to cation exchange or change in entropy, or a mixture of both (Theng, 1982).

Wang et al. (2005) studied the adsorption mechanism of non-ionic guar gum and dansyl-labeled guar gum at different solid-liquid interfaces. Talc was the solid used in the study. The study used total organic carbon analysis and zeta potential to study the extent of polymer adsorption on the surface of talc. There were two main conclusions in this

study: hydrogen bonding was the main driving mechanism behind adsorption because adsorption was reduced by the addition of urea to the solution and that the pH and ionic strength of the polymer solution did not have an impact on polymer adsorption. It is true however, that when polymers are adsorbed and depending on their molecular weight, the end chains will be in a constant process of desorbing and adsorbing. However, the polymer molecules will effectively be adsorbed.

There is a general agreement that the adsorption of charged polymers onto clay surfaces due to cation exchange mechanisms (Theng 1982; Parfitt, 1972). Ueda and Harada (1968) studied the adsorption of diallydimethylammonium chloride-SO_2 copolymer on the surface of bentonite. The authors noted a reduction in the cation exchange capacity of bentonite as a result of polycationic polymer adsorption on the clay surface, indicating that the rock's surface charge was being neutralized over time by polymer adsorption and occupation of cation exchange sites. The amount of polymer adsorbed was calculated from the nitrogen content of the sample. Cation exchange capacity was measured by passing the $NiCl_2$ through a column containing the sample, and then measuring the amount of nickel ions in solution. This measured amount was then converted to cation exchange capacity.

In the case of uncharged polymers, adsorption is due to desorption of water molecules from the surface of the rock, creating enough entropy to cause these polymers to adsorb on the rock surface (Theng, 1982). Parfitt and Greenland (1970) determined that as the

volume of polyethylene glycol adsorbed on montmorillonite increased, so did the volume of water desorbed from the clay surface.

Adsorption also leads to change in the conformation of a polymer structure. The polymer tends to exist as a coil in solutions; when it is adsorbed, it uncoils and spreads on the surface of the rock (Theng, 1982). When polymers with high molecular weight uncoil, they spread over a larger surface area. Therefore, it can be concluded that polymers with high molecular weights adsorb higher than polymers with lower molecular weights.

In addition to the polymer's molecular weight, the degree of adsorption generally depends on the molecular conformation, and electrostatic charge (Letey, 1994). In addition to that, the surface area of the particle, the structure, and pore size distribution of the clay all come into play in determining the extent of polymer adsorption. Theng (1982) explains that the adsorption of polymers by clays increases as the size of the molecular weight of the polymer increases, assuming that surface accessibility is unrestricted. However in clay-water systems as is the case in illite, kaolinite, and montmorillonite, the existence of a porous medium restricts large particles from being adsorbed into the medium beyond the surface.

Schamp and Huylebroeck (1973) monitored the change in polymer adsorption of polyacrylamide by different clay minerals (kaolinite, illite, bentonite, and montmorillonite) as they increased the molecular weight of the polymer. Polyacrylamide was developed by polymerization of acrylamide and the different molecular sizes were obtained by changing the polymerization temperature. The results showed that as the

molecular weight increased, the maximum amount of polymer adsorbed decreased, suggesting that adsorption is only limited by the surface area available on the rock on which it is adsorbed.

Bailey et al. (1994) determined that polymer adsorption is strongly dependent on the ionic nature of the polymer and the ionic strength of the medium. By conducting several experiments on negatively and positively charged high molecular weight polyacrylamide copolymers with negatively charged Wyoming Montmorillonite, they discovered that adsorption of polymers does not occur when there is repulsive force between the clay and polymer. The authors also noted that the adsorption behavior of the polymers studied changed as the concentration of the electrolyte medium (KCl) was increased.

Pawlik and Laskowski (2004) showed that non-ionic guar gum adsorption density on illite was not affected by ionic strength of the background solution, but the amount of polymer adsorbed was significantly reduced when the dolomite was present. It is not entirely clear as to why this type of behavior occurred. At the same time, adsorption of carboxymethyl cellulose (CMC) was dramatically increased as the ionic strength of the medium increased. The study was done by using a temperature controlled shaker, where the minerals were suspended in the polymer solution for 15 minutes, and the solution was essayed for residual guar gum to determine the percentage polymer adsorbed. The viscosity of the polymer was measured with different brine (Lanigan potash ore) concentrations (1%, 25%, and 50%) and found that in all three cases, the viscosity of the

non-ionic guar gum did not change, indicating that non-ionic guar gum does not coil at high ionic electrolyte concentrations.

Saini and Maclean (1966) reported that polymer adsorption of anionic soil polysaccharides on kaolinite was increased with all cations on the order of $Fe^{3+>}Al^{3+}>H^{+}>Ca^{2+}>Mg3^{+}>Na^{+}$, which indicated that the cations were forming complexes with the anionic polymers prior to adsorption. It is expected that non-ionic and cationic polymers would behave differently when exposed to different cations.

Ma and Pawlik (2005) discussed the Hofmeister series of ions as the reason why the presence of brines affects polymer adsorption. The Hofmeister series orders cations from the least to most hydrated ions in the following order: $K<Na<Mg^{2+}$. Small ions are strongly hydrated, with small or negative entropies of hydration, creating local order and higher local density. Since solid surfaces are usually hydrated in aqueous solutions, is it expected that the presence of different metal ions will impact polymer adsorption on those surfaces. The authors studied the adsorption of non-ionic guar gum on the surface of quartz with the addition of different alkali ions. They concluded that (Na^{+} and Li^{+}) acted as structure makers and did not affect adsorption density, while (Cs^{+} and K^{+}) acted as structure breakers and increased the adsorption density of guar gum. The mechanism proposed was that structure breaking ions disturb the water molecules on the surface of quartz, thus providing more space for the polymer to adsorb. It is important to note here that quartz has a cation exchange capacity of zero. Therefore adsorption mechanisms are expected to be different when dealing with charged surfaces.

From the literature described above, it can be concluded that polymer retention (adsorption) depends on the polymer's molecular weight, existence of divalent ions, reservoir temperature, and the cation exchange capacity of the rock.

This thesis discusses the cation exchange capacity of different source rocks and their impact on the adsorption behavior of certain linear polymers on the surface of these rocks. Outcrop samples were collected from the Eagle Ford, Marcellus, and Barnett rocks plus Berea sandstone, crushed into a mean size particles of 0.2 cm, and exposed to linear polymers and a cross-linked gel. Polymer adsorption is one hypothesized fate of one organic additive in fractuting fluid. Additionally, we examine the impact of different brines on polymer adsorption. Finally, we have done some work in order to better understand the breaking behavior of cross-linked gels when contacting different types of source-rocks with varying total organic content (TOC).

2. STATEMENT OF PURPOSE AND OBJECTIVES

Stimulation of sufficient rock volume to produce economic rates and recoveries of hydrocarbons from source rock reservoirs may require injection of upwards of 120,000 bbls of mostly water-based hydraulic fracturing fluid (Penny et al., 2006). Those fluids mainly contain fresh or near-fresh water with polymers, cross-linkers plus other additives (surfactants, biocides, clay stabilizers, etc.) as needed (Montgomery et al., 2010). As discussed in chapter one, these polymers could either be modified guar gum or modified polyacrylamide, depending on the desired function. Both of these polymers are of high molecular weight and complex geometry. Chapter three discusses the different polymers and source rocks used in this thesis, which also includes the methods and procedures used.

Due to the environmental impact of using such large amounts of water – which could alternately be used for life sustaining purpose – it becomes necessary to define methods the industry can utilize to reuse the water that flow back up to the surface after the well is put on-line post fracturing operations (Rassenfoss, 2011). At the same time, care must be taken not to damage the hydraulic fracture conductivity created, which could occur due to the adverse interaction of the rock with the fracturing fluid (Blauch, 2010). Some of the mechanisms of damage from hydraulic fracturing fluids were discussed earlier in chapter one. Also flow-back fracturing fluid must be disposed of in an environmentally friendly manner, which includes the removal of material that could potentially cause any environmental damage (Rassenfoss, 2011). Therefore, the fate of fracturing fluid additives must be clearly understood to learn the source of salinity and scaling tendency changes,

plus the nature of decomposition products from organic additives. Such knowledge will allow us to better address the environmental impacts and potential reuse of fracturing fluid flow-back fluid, as well as determine potential for damage to propped fractures from the interactions between the rock and the fracturing fluids.

The main objective behind this study is to investigate the fate of the organic additives of fracturing fluids as a function of prolonged exposure to rock at elevated temperature and pressure. The additives in question are guar gum and its derivatives and xanthan gum. This study also aims to investigate the whether the interactions between the source rocks and fracturing fluids could alter the behavior of such fluids. This is done by cross-linking the guar gum with borate salt and adding other necessary fracturing fluid additives (pH adjuster, high temperature and low temperature gel breakers, biocide, scale inhibitor, and clay stabilizer).

It has long been hypothesized that the interaction of hydrocarbons with the source rocks they occupy occurs on the molecular level (Sun et al., 2015). Therefore, we hypothesized that the interaction between source rocks and injected fracturing fluids is on the molecular level, as well. Polymer adsorption is one proposed mechanism by which the polymer would adsorb on the surface of the rock due to cation exchange mechanisms. The concept and prior studies are discussed in detail in chapter one. Chapter three discusses the different rock samples and polymers used, as well as their characterization methods and experimental procedure. Further work on polymer adsorption is investigated in chapter four, which includes: discussions on rock and polymer characterization methods,

experiments on the impact of rock properties on polymer adsorption, the impact of polymer properties on polymer adsorption, the impact of brine additives on polymer adsorption, and possible alteration of fracturing fluid behavior as a result of rock-fluid interactions. The chapter also shows detailed characterization of the rock samples studied, which is not only important for this study, but for future studies regarding these source rocks' interactions with injected water-based fluids in those areas. Characterization of the polymers studied is also discussed using fourier transform infrared spectroscopy (FTIR) and rheology.

3. MATERIALS AND METHODS

3.1 Materials

3.1.1 Polymers

Four linear polymers were used in this study: three derivatives of guar gum (a commercial gelling agent, neutral guar gum, and a cationic guar gum) and xanthan gum. Below is a description of the polymers used. The concentration, iconicity, and chemical abstract numbers for each polymer used are summarized in **Table 1**.

Table 1 - Characterization of the polymers used in this study

Polymer	CAS Number	Concentration, mg/L	Iconicity
Cationic Guar	65497-29-2	5000	Cationic
Guar Gum	9000-30-0	3200	Neutral
Xanthan Gum	11138-66-2	1175	Non-ionic
Commercial Oilfield gelling agent	Proprietary	2500	Unknown

Guar gum is natural polymer that is extracted from of the plant cyamopsis tetragonalobus (Gupta and Arora, 2012). The chemical composition of the polymer is a galactose to mannose ratio of 1:2, which consists of a (1-4) linked β-D mannopyranosyl backbone, partially substituted at O-6 with a D- Galactopyranosyl side groups (Gupta and Arora, 2012). The structure of a single repeating unit of guar gum is shown below (**Fig. 2**) where the letter "n" refers to the number of repeating units that compose the entire

polymer chain. Each polymer molecule contains nine hydroxyl groups, which are responsible for the polarity of the polymer (Tiraferri et al., 2008).

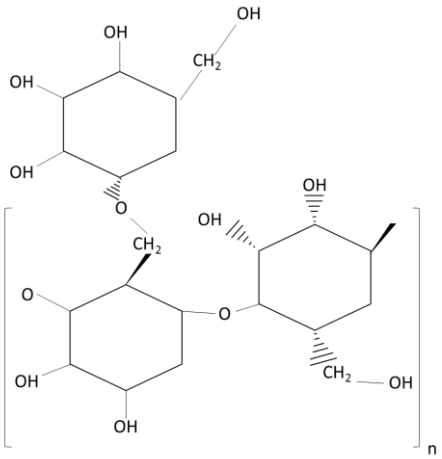

Fig. 2: Guar gum monomer showing the (1-4) linked mannopyranosyl and D-galactopyranosyl (adabted from Gupta and Arora, 2012).

Mechanically, the polymer is resistant to thermal degradation (pH of 3 at 122 F°) (Avachat et al., 2011). Generally, the polymer is used as a viscosifier in several applications, including the oilfield. Guar gum is used in hydraulic fracturing applications as a gelling agent to increase the proppant carrying capacity of water.

Raw guar gum is non-ionic and can be modified in different ways to achieve a specific purpose in addition to its viscosifying effect. Guar hydroxypropyltrimonium chloride is a modified guar gum that is used as a conditioning cationic polymer. This polymer is derived from native guar with N-(2,3-epoxypropyl)-N,N,N-trimethylammoniom chloride,

which results in a cationic polymer (Ungewiβ et al., 2005). Commercially, cationic guar is used as a conditioning agent in cosmetic hair products.

Xanthan gum is a biopolymer synthesized from the bacterium *Xanthamonas Campestris*. The importance of xanthan gum is due to its remarkable rheological properties. The polymer is capable of achieving a 100,000 times increase of water viscosity at low shear rates, but only 10 times increase of water viscosity at high shear rates (Whitcomb and Macosko, 1978). Very few other polymers have this pseudo-elastic capability. The uniqueness of xanthan gum comes from a trisaccharide side chain on alternate sugar units. This unit is composed of glucuronic acid (COO^- group) salt between mannose acetate and a terminal mannose unit (Adhikary and Singh, 2004). There is a pyruvate unit that is attached to the molecule, which together with the glucuronic acid give xanthan gum its anionic charge. This could be neutralized by addition of different ions, such as potassium, calcium, and sodium. Below is the chemical structure of xanthan gum (**Fig. 3**).

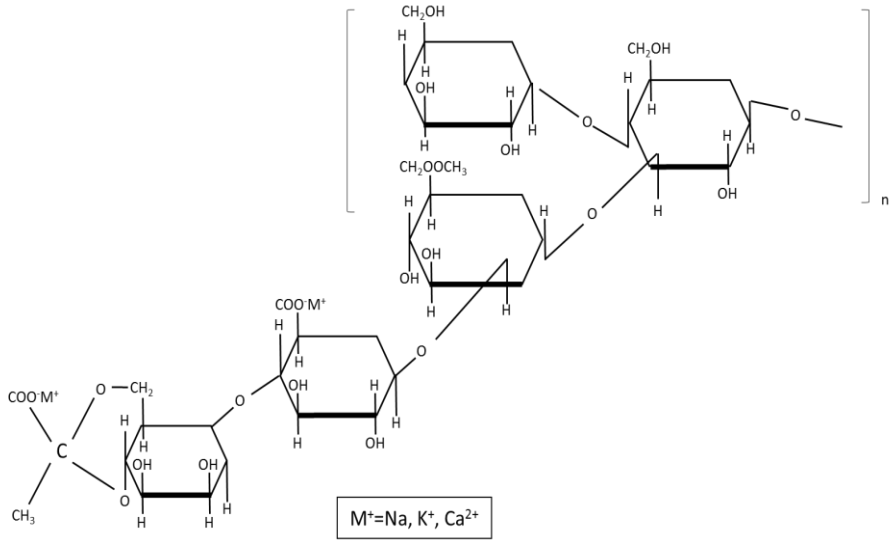

Fig. 3: Xanthan gum monomer (adabted Adhikary and Singh, 2004)

Xanthan gum has been used in the oil and gas industry as a viscosifier in drilling, well stimulation, well completion, and enhanced oil recovery applications (Khan et al., 2003). The reason behind this diverse use of the polymer comes not only from its unique rheological ability, but also from its stability under a wide range of saline and temperature environments (Khan et al., 2003).

3.1.2 Fracturing Fluid Components

Different fracturing fluid components were supplied by an oilfield services company, the contents of which and corresponding concentration per 1 mL of water are shown below (**Table 2**).

Table 2 - Fluid additives per 1 mL of water

Additive	Amount (per 1 mL)
Gelling Agent	0.003g
Biocide	0.001893mL
Surfactant	0.001893mL
Gel Stabilizer	0.00757mL
Clay Stabilizer	0.003875mL
High Temp Breaker	0.00012g
Low Temp Breaker	0.00006g
pH Adjuster	0.003875mL
Cross-linker	0.005678mL

3.1.3 Rock Samples

Three source rock samples plus Berea Sandstone core plugs were used in this study. Those samples were selected because of their importance to the oil and gas industry as well as their diverse geochemical composition. Below is a description of each sample:

The Barnett Shale play is located in the Fort Worth Basin of north-central Texas. The play covers a large geographic area and is considered to be one of the most uniform stratigraphic units in the Basin. In a study performed by Kale et al. (2010), the rock was determined to contain a total organic content (TOC) ranging from 1% to 15% and clays from 20% to 45% with illite being the dominant clay. The study also reported that trace amounts of smectite can also be found in the Barnett Shale. Intially when the play was first discovered, fracturing stimulations were carried out by pumping large amounts of proppants supported by cross-linked gelled fluids. As new advances in hydraulic fracturing were introduced, the industry eventually moved to using slick-water fracturing

to reduce cost and improve conductivity (Penny et al., 2006; Frantz et al., 2005). Typical fracturing stimulation operations in the Barnett Shale utilize about 1 MM gallons of water, with 30% to 40% of the injected water returning to the surface after the well is put on production (Penny et al., 2006). The outcrop collected for this study is located in San Saba, TX in the United States.

The Marcellus Shale is the most extensive source rock-gas play in North America, spanning 95,000 square miles across the Northeastern Continental US. TOC ranges from 3% to 6% as reported by Belvalkar and Oyewole (2010). Clay content for the Marcellus shale ranges from 10% to 35% by weight percent of the rock (Bruner and Smosna, 2011). A typical fracturing operation in the Marcellus utilizes about 540 M gallons of slickwater fluid (Fontaine, 2008). Approximately 10% to 30% of the water used to stimulate the well returns to the surface (Rassenfoss, 2011). Outcrop rocks were collected in Pennsylvania in The United States.

The Eagle Ford Shale is one of the most prolific source rock plays in the US; it produces oil, gas condensate, and dry gas (Tian et al., 2013). According to Mullen et al. (2010), the Eagle Ford Shale has long been known as the source rock for the Austin Chalk, and is currently being developed as a self-sourcing rock. Current geological descriptions classify the Eagle Ford shale as two layers: an upper carbonate – rich and a lower clay-rich. The total organic content (TOC) ranges from 2% to 6% (Mullen, 2010). The reservoir is predominantly composed of calcite ranging from 40% to 70% (Mullen et al., 2010) and total clay content, ranging from 5% to 46% (Mullen, 2010). Hybrid fracturing is currently

the predominant fracturing technology in the Eagle Ford (Yang et al., 2013). Hybrid fracturing uses a combination of friction reducer, a gelling agent, and one or more cross-linkers in order to transport proppant into a hydraulic fracture. A typical fracturing treatment in the Eagle Ford shale utilizes over 4.2 MM gal of water (Yang et al., 2013). Outcrop samples for this study were collected from the lower part of the upper Eagle Ford Layer in Del Rio, TX in The United States. The location of this outcrop is a site of several studies that are currently being conducted on the Eagle Ford Shale.

In addition to the three types of source rocks, Berea sandstone samples were also studied to develop baseline experiments to better understand how the polymers interacted with a rock that had significantly low clay content, total organic content, and cation exchange capacity.

3.2 Methods

3.2.1 Determination of Mean Particle Size

The experiments were conducted on crushed samples. Before the experiments were conducted, a particle size distribution was obtained using a standard sieve analysis (**Fig. 4**). The figure shows cumulative percentage retained on a phi (ϕ) scale. The mean size of the particles was determined using **Eq. 1**:

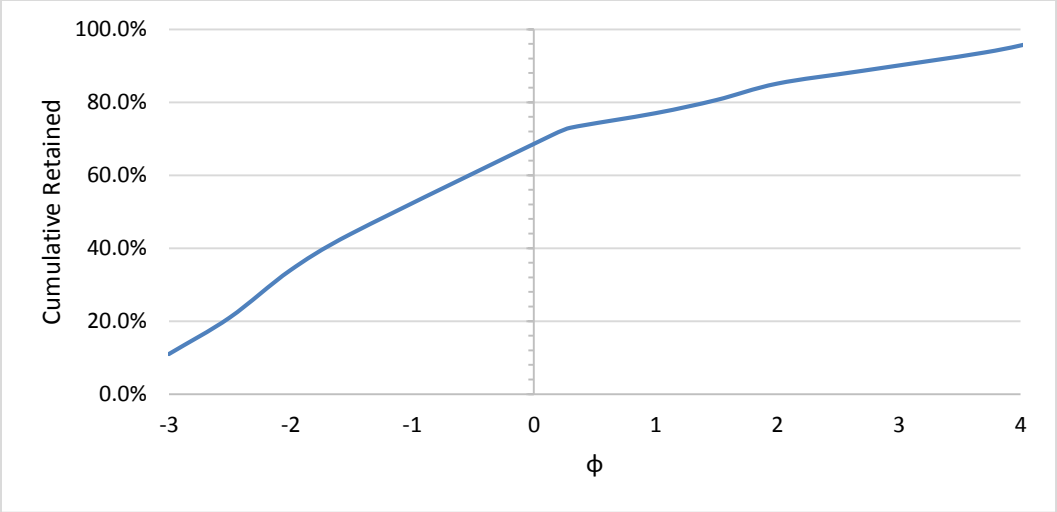

Fig. 4: Cumulative distribution of the particle size of crushed rock on a phi scale

$$\text{Graphic Mean} = \frac{\text{D10} + \text{D50} + \text{D84}}{3} \ldots\ldots 1$$

where D10, D50, and D84 refer to the particle diameter in phi scale at 10% retained, 50% retained, and 84% retained, respectively. **Table 3** summarizes the results and the graphic mean is -0.85. This value is roughly 0.2 cm.

Table 3 - Summary of mean particle size determination

Particle Diameter	% Retained
D10	-3.1
D50	-1.2
D84	1.7

3.2.2 Static Experiments

The laboratory apparatus consist of a metal aging cell, with a protective Teflon® liner enclosed on the inside. The inside of the liner is completely isolated from the cell using a Teflon® lid with a screw-in cover. The aging cell is covered with a metal lid with an orifice for gas injection and/or vacuum. A roller oven with an adjustable thermostat is used for the experiments (**Fig. 5**).

A – Tephlon Liner

B – Aging Cell Setup

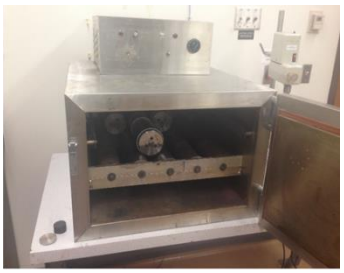

C – Roller Oven

Fig. 5: Experimental setup

A 1000 mL tap water sample at 100 °F is taken and placed inside a clean, dry blender. A reading of pH of the water is taken and adjusted to a range between 7 and 7.5 using 15% by weight HCl. This helps ensure that the polymer is properly hydrated. The blender is then turned on and the voltage is increased until a vortex is formed on the bottom of the blender. This is done to make sure that enough shear is created, which does not break the polymer chain. The required polymer concentration is then added to the water, making sure the vortex remains on the bottom of the blender. The resulting polymer solution

should hydrate after approximately 10 to 15 minutes. Full hydration of the polymer solution is ensured by ontinuous viscosity sampling of the solution until a constant viscosity reading is obtained (35-45 cP). An initial viscosity measurement is recorded as the initial viscosity (μ_i). During the preparation of the polymer solution, the oven is turned on and set to 115 °F. This temperature was selected to inhibit the thermal degradation of the polymer solution. The polymer solution is then set aside until rock preparation is complete. The rock sample is weighed to 70 grams and placed inside the Tephlon® liner, then the polymer solution is poured inside the liner. The resulting mixture is then stirred using a clean disposable spoon to ensure homogeneity. The Tephlon® lid is then fully inserted into the liner until it barely touches the surface of the mixture. The liner is then placed inside the metal aging cell, which should be checked for the presence of all the required seals and o-rings. Replacement parts should always be present in the lab in-case of any missing part. The cell is then covered with the provided lid and purged with nitrogen gas up to 100 psi to prevent aerobic bacteria from developing inside the cell and to simulate subsurface conditions. In order to make sure there are no leaks in the system, the cell is placed inside a water bath and checked for the presence of air bubbles. If any bubbles are coming out, the cell should be opened and o-rings replaced, repeating the steps above. After the cell is pressurized and checked for leaks, it is then placed inside the roller oven. The roller is then turned on for 30 minutes to allow the mixture to homogenize. The roller is then turned on and off again for 30 minutes at six hour intervals. The system is allowed to react for 24 hours, which is then depressurized, and the solution is removed

using a transfer pipette and placed aside until it returns to room temperature. The broken solution's viscosity is measured using a Brookfield Viscometer with a standard LV-1 Spindle at 20 rpm. Finally, the percent viscosity reduced is calculated using **Eq. 2**

$$\%\text{Reduction} = \frac{\mu_i - \mu_f}{\mu_i} \ldots\ldots 2$$

The preparation procedure of the cross-linked borate fluid is similar to the preparation method of the linear polymer. However, different components are also added to the solution while in the blender at one minute interval each. The components are in the following order: biocide, gel stabilizer, clay stabilizer, pH adjuster, low temperature breaker, high temperature breaker, and cross-linker. In order for the gel to fully cross-link, it should be kept in the mixer two to three minutes after adding the cross-linker. At the end of the mixing process, the gel should exhibit a lipping behavior (**Fig. 6**). Ingredients for 1 mL of water solution are shown in materials section in **Table 2**. This receipe could be adjusted for different gel volumes. The fluid and crushed rock sample are placed inside the liner and into the aging cell in a similar manner as the linear polymer solution experiments, and placed in the oven at 200 °F. This temperature is necessary for the gel breaker to properly activate. At the end of the experiment, the cell is depressurized and the fluid is separated from the rock. The solution's viscosity is then measured using a Brookfield Viscometer with a standard LV-1 Spindle at 20 rpm.

Fig. 6: Guar-based cross-linked gel

3.2.3 Source Rocks Samples Characterization

The rock samples were characterized using soil characterization methodologies, which are x-ray diffraction, thermogravimetric analysis, cation exchange capacity, and pH.

X-ray diffraction was used to determine the mineralogy of all four samples, which is a technique that is used to provide information about the structure of crystalline substances. When x-rays are directed towards a rock sample, the x-rays will scatter according to a specific pattern, depending on the mineralogical composition of the rock (Harris and White, 2008). This pattern in addition to its intensity is used to identify the mineral. This analysis was done at a commercial lab using a Bruker Endeavor D4 x-ray Diffractometer. The mineral identification was performed in JADE V. 9.5 software. The quantitative analysis was performed by the Reitveld method with no accounting for any

amorphous phase. The results are normalized to 100% based on the assumption that the complete mineral content of the sample is accounted for in the XRD patterns. A complete explanation of the sample preparation can be found in appendix A.

Thermo-gravimetric analysis (TGA) was used to determine the total organic content (TOC) of the samples. The samples were ground and sieved through a 10 micron sifter. The heating rate was determined to be 3 °C/min as obtained from Easley et al. (2007) and the analyses were conducted under air injection up to 900 °C.

Cation exchange capacity: measures the tendency of the rock surface to attract positively charged particles. Soils containing clays and organic matter are negatively charged by nature. These negatively charged soils attract and hold on to cations using electrostatic forces (Ross and Ketterings, 2011). The analysis was done using the pH 7.0 ammonium acetate procedure of Chapman (1965) at the Soil Characterization Laboratory. A detailed description of the procedure can be seen in appendix A.

The pH of the Barnett, Eagle Ford, and Marcellus samples were calculated using a soil reaction method by mixing the ground rock with distilled water and stirring it at 15 minute intervals for about an hour, then measuring the pH of the solution.

3.2.4 Polymer Characterization

The polymers were characterized to qualitatively determine their molecular characteristics and rheologic nature using fourier transform infrared spectroscopy (FTIR) and viscosity measurements, respectively.

Fourier transform infrared spectroscopy (FTIR) was used to qualitatively determine the differences in the molecular structure of the four different polymers (King et al., 2004). The analysis was done using a Cary 630 FTIR Spectrometer on the polymers in their solid powder form.

Rheology of the polymer solutions was also studied using a Brookfield DV-III Ultra viscometer with a standard LV-1 spindle measured at 20 rpm. This was done to understand the nature of the polymers while hydrated in water and 2% metal ion solutions.

4. RESULTS AND DISCUSSION

4.1 Rock Characterization

Rock mineralogy with x-ray diffraction was performed on three source rock samples plus the Berea Sandstone. **Table 4** shows the mineralogical analysis for each source rock sample.

Table 4 - Mineralogical analysis of the Barnett, Marcellus, Eagle Ford shales and Berea sandstone

Mineral	Barnett	Marcellus	Eagle Ford	Berea*
Smectite	0	2	0	1
Chlorite	4.0	Tr	0	0
Kaolinite	5	0	7.2	4
Illite/Mica	32.0	16.0	1	Tr**
Mx IS	9.0	7.0	0.9	0
Calcite	Tr	12	60.1	0
Dolomite	0	1	4	0
Quartz	31	41	20.2	91
K-Feldspar	2	2	0	3
Plagioclase	2	6	0	1
Pyrite	1	12	5.2	0
Barite	0	0	0	0
Fluoroapatite	11	1	0	0
Gypsum	3	0	5.4	0
Clays	50	25	9.1	5
Carbonates	0	13	60	0
Other	50	62	30.8	95

*Values obtained from Kocurek Industries **Tr:trace

The analysis shows that the Barnett shale has very high clay content, comprising 50% by weight of the total mass of the rock. We can see that illite/mica content is high. The

other half of the rock is mainly quartz and fluoroapatite. The Marcellus shale shows less clay content at 25% of the mass of the rock. Some carbonates are present at 13%. Finally, the Eagle Ford shale shows the lowest clay content of the three with 9.1% and calcite comprises the majority of the rock at 60% of the mass of the rock.

The effective surface area for each sample was calculated based nominal relative surface areas for each clay based obtained from Civan (2007) shown in **Table 5**. It is important to note that the calculations below only take into account the clay content of the rock – not taking into account its total organic content – because the relative surface area of kerogen – which makes up the organic content of those source rocks – is very small compared to illite or smectite. **Table 6** shows the effective surface area for each rock type, calculated by considering only the clay content of these rocks.

Table 5 - Reported surface area for each clay type (Civan, 2007)

Clay	Surface Area, m^2/g
Smectite	700
Chlorite	100
Kaolinite	20
Illite	100
Mx IS	400

Table 6 - Calculated surface area of each sample based on the clay content

Rock type	Effective surface area, $m^2/100g$
Barnett	51.1
Marcellus	40.6
Eagle Ford	.042
Berea	.056

The pH of the Barnett, Eagle Ford, and Marcellus shales was calculated using a soil reaction method by mixing the ground rock with distilled water and stirring it at 15 minute intervals for about an hour, then measuring the pH of the solution. The results are shown below (**Table 7**)

Table 7 - Measured pH values for three source rocks

Sample	pH
Barnett	4.7
Marcellus	7.7
Eagle Ford	7.5

The results show the Barnett as moderately acidic, while the Eagle Ford and Marcellus are neutral. The low pH of the Barnett could be attributed to the occurance of chemical weathering processes given the fact that outcrop samples are being used in this study. The neutrality of the Eagle Ford is due to the presence of calcite (60% by weight) in the sample, which neutralizes the pH of solution. The presence of 13% by weight carbonate in the Marcellus also contributes to the neutrality of the sample.

Cation exchange capacity (CEC) of samples was determined according to Chapman (1965) and the results were further validated by calculating the cation exchange capacity of the clays for each sample using values obtained from the literature (Carroll, 1959) shown in **Table 8**. **Table 9** summarizes the results, which include calculated cation exchange capacity values by taking the average of the range provided for each clay type in **Table 8**. It is important to note here that the cation exchange capacity of mixed-layer

illite/smectite was not taken into account in this calculation because the ratio of illite to smectite was not known. The measured cation exchange capacity for Eagle Ford is shown to be outside of the calculated range. It is worth nothing that the ammonium acetate procedure is valid when dealing with rocks that contain mostly clays and relatively insoluble components, such as quartz and feldspar (Dohrmann, 2006). The partial dissolution of Ca^{2+} is added to the dissolved exchangeable ions, which could lead to highly erroneous CEC values, as is the case in the Eagle Ford shale (Dohrmann, 2006). The low pH of the Barnett sample – as shown in **Table 7** – might cause the cation exchange capacity measurements for this rock to deviate from the actual value (Ketterings and Ross, 2011). Again, we note here that the cation exchange capacity is only calculated based on the clay content of the sample.

Table 8 - Cation exchange capacity for each clay type (Carroll, 1969)

Clay	Cation Exchange Capacity, meq/100 g
Kaolinite	3-15
Chlorite	10-40
Illite	10-40
Smectite	80-150

Table 9 - Cation exchange capacity measured and calculated

Sample	Measured, Meq/100 g	Calculated, Meq/100 g	Average Calculated, Meq/100 g
Barnett	18.7	3.75 – 15.15	9.45
Marcellus	5.3	3.2 – 9.4	6.3
Eagle Ford	4.5	0.316 – 1.48	0.898
Berea	0.03*	0.92 – 2.1	1.51

*This value was not measured but adapted from Lowe et al. (1999)

Total organic content of the rocks was determined using thermos-gravimetric analysis. **Fig. 7** shows the weight loss curve for each sample with an increase in temperature.

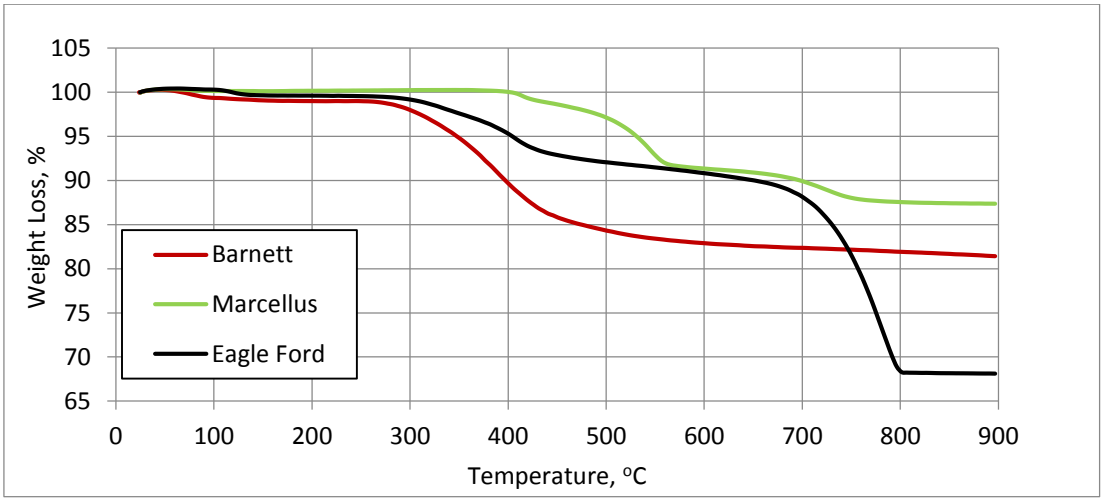

Fig. 7: Heating curves for the three types of rock used in this study by TGA

Weight loss up to approximately 100 °C can be attributed to moisture loss and loss of interlayer water from clay minerals (Speight, 1999). The Barnett shale shows the highest weight loss, which can be attributed to the higher clay content of the rock. Clays usually

hold a significant amount of clay-bound water. Weight loss from 300 °C to 450 °C is loss of the organic matter (Kerogen) (Speight, 1999). Kerogen is an insoluble organic matter that occurs naturally in source rocks, and can yield oil upon heating. Typical constituents of the kerogen are algae and woody plan material. It is important to note that the weight loss of the kerogen is a one-step decomposition. This type of decomposition has been demonstrated by other work on oil shales (Aboulkas and Harfi, 2008). The importance of this property is to distinguish decomposition of kerogen from other organics that might be present in the rock. Heating above 450 °C caused the decomposition of minerals due to the presence of carbonates, which can be see clearly in the Eagle Ford Sample (Burger et al., 1985). **Table 10** shows the results of the TGA analysis.

Table 10 - TGA results for three rock samples

Sample	Moisture	Organic Decomposition	Organic Content	Transition zone	Inorganic content	Inorganic decomposition
Barnett	3%	300-500 °C	15%	N/A	N/A	N/A
Marcellus	1%	300-550 °C	7%	550-700 °C	13%	770 °C
Eagle Ford	1%	300-420 °C	6%	420-700 °C	24%	800 °C

4.2 Polymer Characterization

Fourier Transform Infrared Spectroscopy: FTIR measurements were conducted using a Cary 630 FTIR Spectrometer on the polymers in their solid powder form. **Fig. 8** shows

the IR spectra of three of the polymers used. Observing the peaks between 800 $cm^{-1}$and 1200 cm^{-1} (fingerprint region) indicate the presence of highly coupled C-C-O, C-OH bonds that represent the polymer backbone (Mudgil et al., 2012). This region correspond to the effect of α and β forms of galactose, mannose, and glucose. A comparison between the absorbance intensity of this band in the different polymers that were studied could reflect the different mannose/galactose (G/M) ratios present in each polymer (Belea et al., 2005). G/M ratio does have an impact on viscosity in that polymers with low G/M ratio have lower viscosities when compared to polymers with high G/M ratios (Issarani and Nagori, 2005). By comparing the three polymers, we can see the Gelling agent has the highest peak, while xanthan gum and neutral guar show similar absorbance intensities. Cationic guar is shown to have the lowest absorbance. It is interesting to note here that the polymer concentration needed follows closely the peak intensities of the polymers in the fingerprint region (it takes almost twice as much cationic guar as the gelling agent to reach a similar viscosity).

The presence of water molecules at around 1600 cm^{-1} can also be observed in all three polymers. The larger absorption band in the neutral as compared to the cationic guar could justify improved solubility in water (Mudgil et al., 2012). It is worth noting here that the cationic guar normally takes twice as long to fully hydrate as the gelling agent.

Glucuronic acid, the signature group for xanthan gum, causes the C=O stretch around 1700 cm^{-1}. Finally, the O-H stretch around 3300 cm^{-1} can be seen with varying degrees of absorbance intensity for different polymers. This stretch is due to the O-H stretching

vibrations of the polymer and water molecule involved in hydrogen bonding (Ping et al., 2001). The high O-H stretch peak of the gelling agent and its high water content (shown at 1642 cm^{-1}), coupled with the fact that it could be cross-linked using borate, show that this gelling agent might be some form of a hydrolyzed guar gum. Mudghil et al. (2012) does show that partially hydrolyzed guar gum has a higher absorbance in the O-H stretch region than native guar gum. The difference in peak intensities between the different polymers themselves is probably due to the way the monomers were repeated to form the polymer molecule.

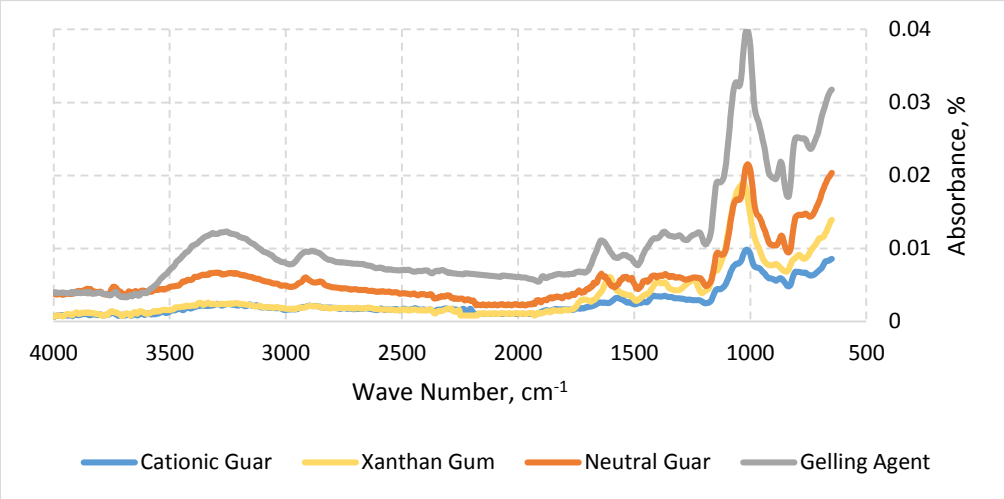

Fig. 8: IR spectra of four different polymers

Rheological Properties: The rheological properties of the four polymer studied, hydrated with fresh water are shown in **Fig. 9** and **Fig. 10**. Viscosity (cP), shear rate (sec^{-1}), and shear stress (N/m^2) readings were taken. **Fig. 9** shows that all three guar polymers behaved

as Newtonian fluids due to the linear relationship between shear stress and shear rate. Xanthan gum is shown as pseudo-elastic with a shear-thinning behavior. However, **Fig. 10** shows that guar gum does behave as shear-thinning, as well. Shear rate is the speed of deformation of the polymer solution in the shear mode, while shear stress is the measure of the force of friction resulting from a fluid acting on a body in the path of that fluid (Wang and Dealy, 2013)

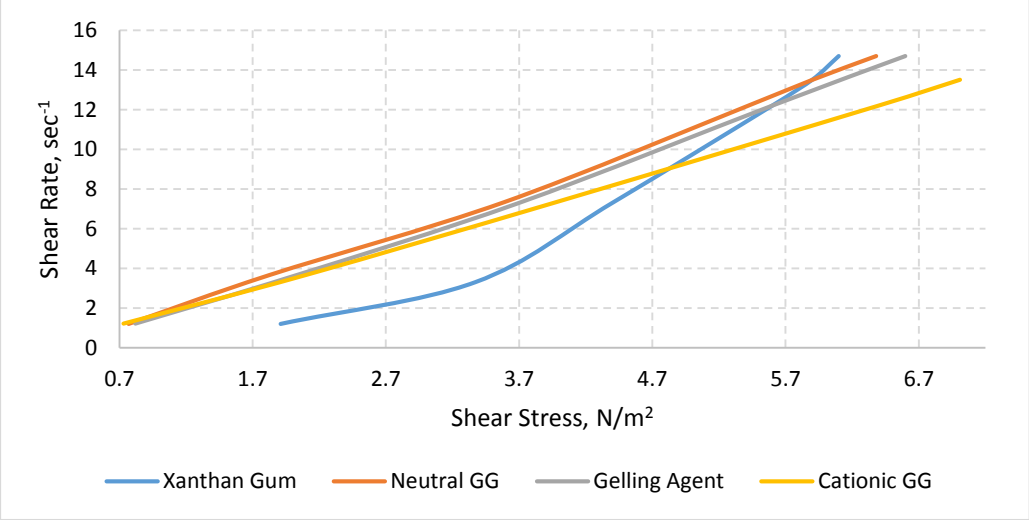

Fig. 9: Shear stress vs. shear rate of four different polymers

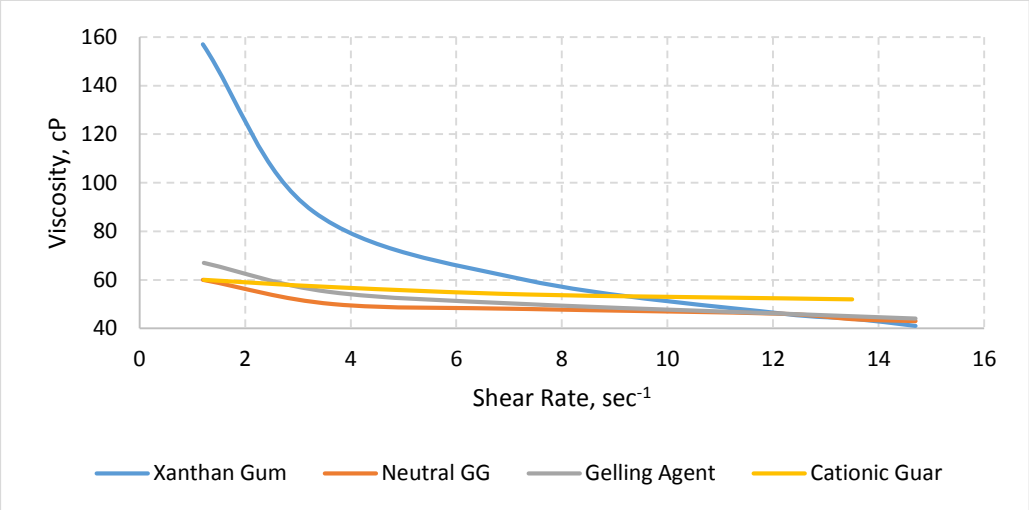

Fig. 10: Shear rate vs. viscosity of four different polymers

4.3 Impact of Rock Properties on Polymer Adsorption

The interaction of the commercial gelling agent and three linear polymers with the Barnett, Marcellus, Eagle Ford Shales, and the Berea Sandstone are shown in **Fig. 11**. A batch fluid was prepared and exposed to the four different rocks in each experiment. A constant initial viscosity value for each batch experiment could not be obtained. Therefore the final viscosity values were converted to percent reduction from the original viscosity (30-45 cP). A blank sample is a polymer that is placed in the oven under the same conditions (Pressure, temperature) as the other samples, without exposing it to any rock fragments.

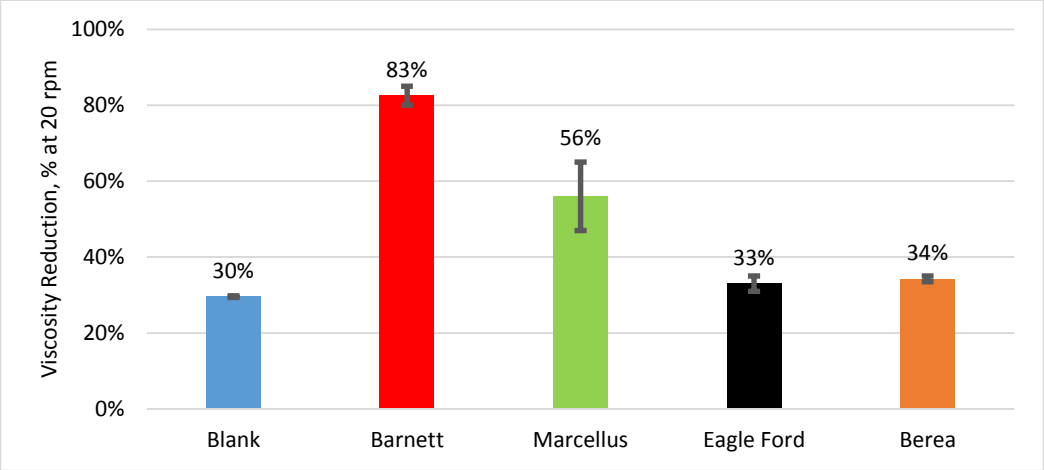

Fig. 11: Reduction in the viscosity of linear polymer after exposing it to different rock samples.

Note that the highest surface area (51 m^2/100 g rock) has been calculated for the Barnett Shale, then for the Marcellus, and the lowest is the Eagle Ford (**Table 6**). Hence there is a correlation between the calculated surface area and viscosity reduction (**Fig. 12**). Moreover, a correlation is also found between **Table 9** (CEC) and viscosity reduction (shown in **Fig. 11**). The correlation is presented with a good linear relation below (**Fig. 13**).

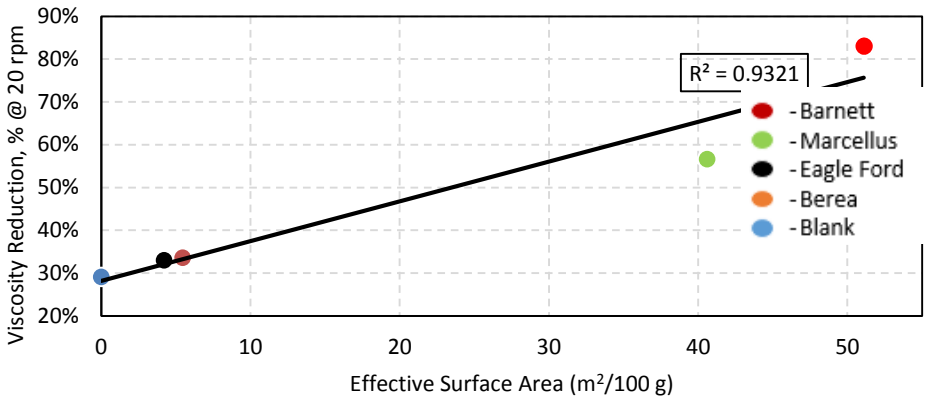

Fig. 12: Correlation between the effective surface area (m^2/100 g) and viscosity reduction.

The same approach was followed to correlate the viscosity reduction to the cation exchange capacity of the rock. Shown in **Fig. 13** are the results, with an R^2 value of 0.88. Deviation in this data might due to the errors encountered in calculating the cation exchange capacity as explained above.

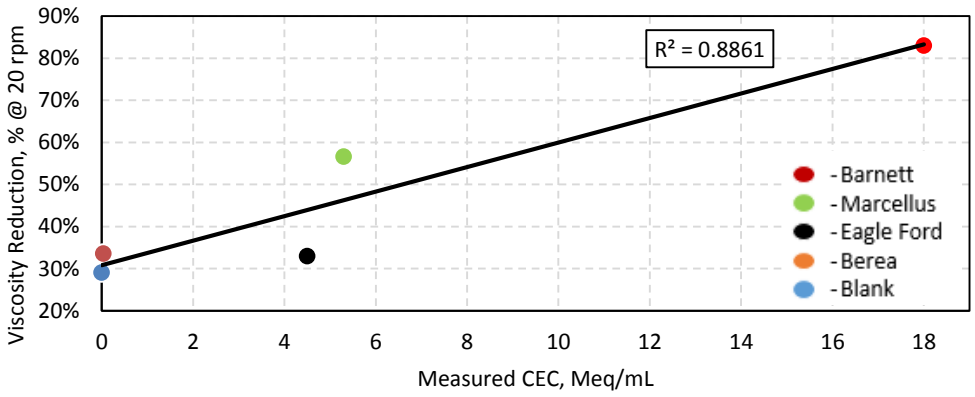

Fig. 13: Correlation between the measured cation exchange capacity (meq/mL) and viscosity reduction.

Because of this potential for error, the same plot was made using the average values of the cation exchange capacity (**Table 9**) as calculated based on the clay content of each rock and it has been observed that the calculated CEC correlates better with viscosity reduction than the measured values (R^2 of 0.97). The results are shown below (**Fig. 14**). Both **Fig. 13 and Fig. 14** show that the adsorption behavior of the polymer is influenced by the polar nature of the polymer (shown in **Fig. 8**) and the cation exchange capacity of the clays (Parfitt, 1972).

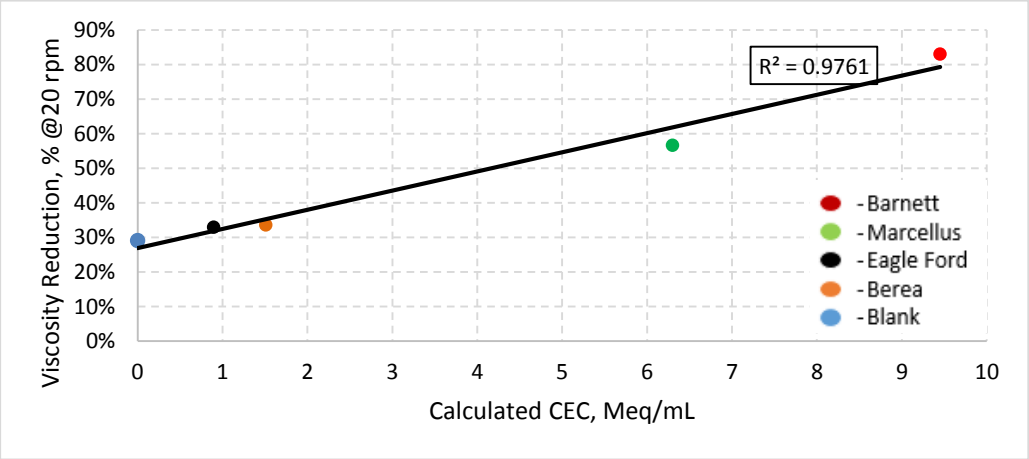

Fig. 14: Correlation between the calculated cation exchange capacity (meq/mL) and viscosity reduction.

We would like to know if such adsorption might be significant in a field hydraulic fracture case. Using some assumptions we can derive an approximate ratio of rock surface area to fluid volume used. As stated earlier, the mean particle size of rock samples in the experiments is 0.2 cm. Assuming that all particles are spheres of 0.2 cm diameter, we can

compute a surface area of 0.1256 cm^2 and volume of 0.00418 cm^3 for each particle. Using a nominal rock density of 2.5 g/cm^3 (Manger, 1963), the mass of each particle is 0.0104 g. Each experiment used 70 grams of crushed rock, so by dividing the total mass of the sample by the mass of a single particle, the total number of particles is determined to be 6866. Multiplying the surface area of a single particle by the total number of particles, the total surface area is calculated to be approximately 840 cm^2. Given that the total fluid volume used in the experiment was 100 mL, the ratio of the total rock surface area to the fluid volume used is approximately 8.4 cm^2/mL. The actual ratio is probably higher than this due to non-sphericity and varying sizes of the real particles. The same calculation was made assuming all cubes (11.61 cm^2/mL) and half of the mass as cubes and half as spheres (4.98 cm^2/mL). By equating the surface area of a sphere to the surface area of a cube (**Eq. 3 and Eq. 4**), we are able to calculate the length of one side of the cube (1.44 mm).

$$4 * \mathrm{pi} * r^2 = 6 * x^2 \ldots\ldots 3$$

$$x = \sqrt{\frac{4}{6} * \mathrm{pi} * r^2} \ldots\ldots 4$$

Where r is the radius of the sphere and x is the length of the side of a cube. Using the same workflow described above in this section, the ratio of the total rock surface area to the fluid volume is 11.61 cm^2/mL. Similarily , the half spheres-half cubes is calculated to be 10 cm^2/mL.

We would like to know if this ratio is reasonably close to that expected in a hydraulic fracture created in the field. While there is undoubtedly variation in fracture widths, a

nominal width of 0.10 cm is considered reasonable (Ramurthy et al., 2011). Assuming a smooth face in a fracture element of 1.0 x 1.0 cm, the total fracture surface area is 2 x 1.0 cm^2 or 2.0 cm^2. The volume of fracture fluid between the faces of this fracture element is essentially 0.10 mL (**Fig. 15**). This yields a rock surface area to fluid volume ratio of 20 cm^2/mL. Recognizing that these calculations rely on assumptions that may be in error, we nevertheless conclude that – for linear gels where the polymer is of similar molecular weight to those used here – significant losses of polymer to rock surface may very well occur in a field fracture case.

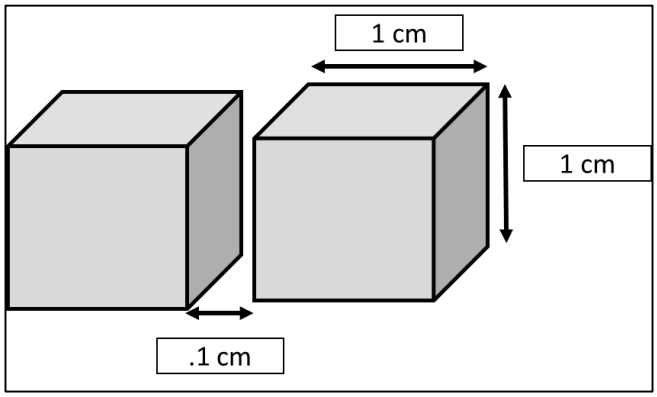

Fig. 15: Fracture surface with 0.1 cm fracture width

Initially, it was believed that the 30% reduction in viscosity in the blank solution was due to bacteria developing in solution during period when the blank was placed in the oven. Therefore, an experiment was conducted with, and without the presence of biocide in solution to rule out the effect of bacteria. Three solutions were prepared with the gelling agent polymer; a polymer solution with no biocide and two polymer solutions with .2%

biocide (25% H_2O Gluteraldyhide from Sigma Aldrich). The no-biocide polymer solution and one of the biocide polymer solutions were placed in aging cells, purged with nitrogen gas, and placed in the roller oven for 24 hours, while the third solution was left exposed to air under room conditions. **Fig. 16** shows that only about 3% of the viscosity reduced was possibly due to bacteria, while no viscosity reduction was observed in the third blank solution (biocide polymer solution exposed to air). This indicates that the viscosity reduced in the blank solution occurred inside the aging cell. And since the cell was lined with a Tephlone® liner, which has virtually zero cation exchange capacity, we ruled out the fact that some of the polymer adsorbed on the liner's wall. This leaves thermal degradation of some of the polymer as the most likely mechanism behind the majority of the 30% reduction. Reservoir temperature in the source rocks studied varies from 130 °F in the Marcellus, to 200 °F in the Barnett, and 350 °F in the Eagle Ford (Chaudary, 2011; Cipolla et al., 2010; Husain et al., 2011). Therefore we expect that some thermal degradation to occur to the polymer as a result of this difference in temperature (experimental *vs.* reservoir). The same experiments were performed at higher temperatures (250 °F) and the results are shown in **Fig. 17**. Since the blank sample shows 71% viscosity reduction, we conclude that thermal degradation is the dominant degradation mechanism over adsorption at high temperatures. For this reason, we expect that the polymers will thermally degrade in the Barnett and Eagle Ford formations more so than be adsorbed.

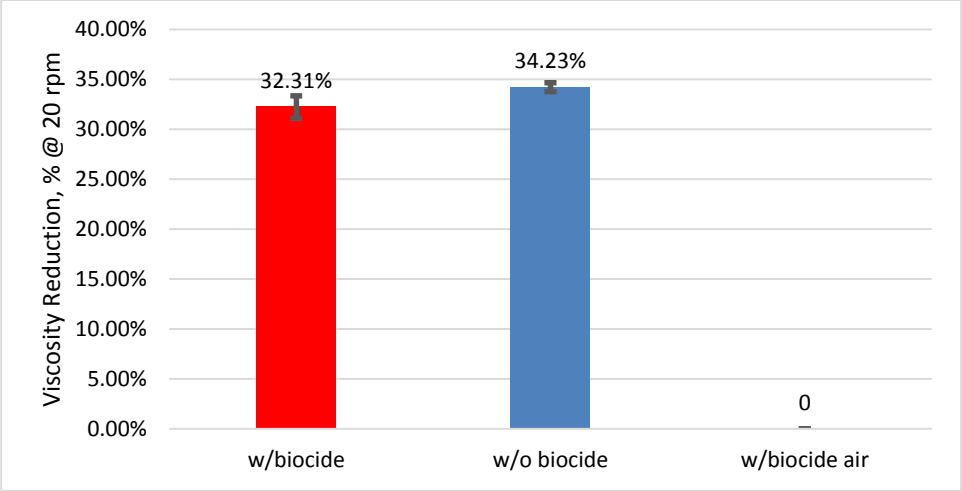

Fig. 16: Biocide (gluteraldehyde) has a little impact on viscosity reduction

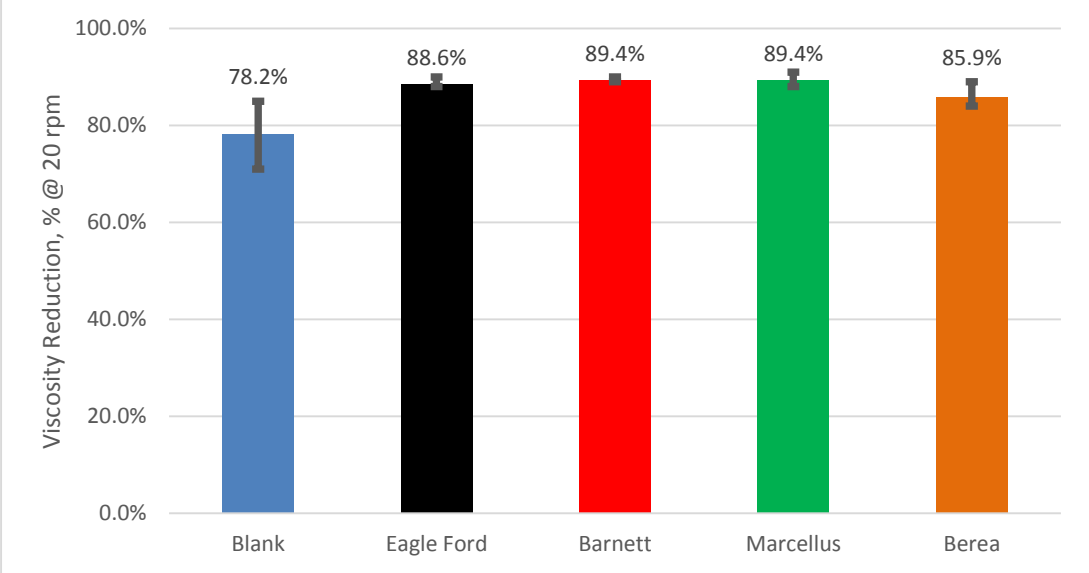

Fig. 17: Thermal degradation of the polymer is the dominant mechanism when compared to polymer adsorption.

4.4 Impact of Polymer Properties on Polymer Adsorption

To further investigate this adsorption behavior, Barnett shale samples were exposed to three different linear polymers: cationic guar, neutral guar, and xanthan gum, in addition to the commercial gelling agent. It is worth noting here that the neutrality of the neutral guar was not verified from a trusted source. For consistency, the final viscosity values were converted to percent viscosity reduction from the initial viscosity (**Fig. 18**).

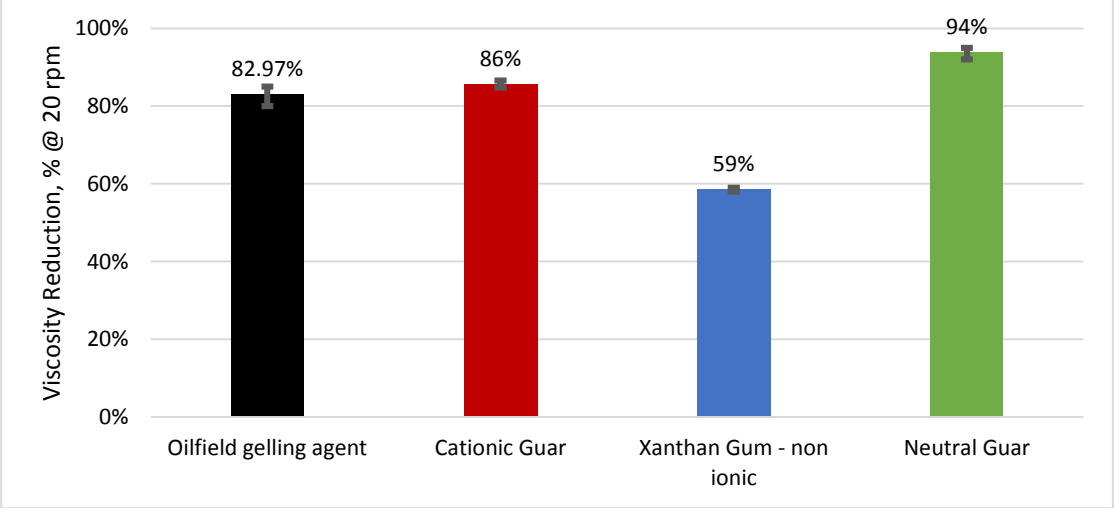

Fig. 18: Viscosity reduction of four different linear polymers after being exposed to Barnett shale outcrop for 24 hours at 115 °F. Average values of three experiments are shown with standard error bars

From the above results we can see that xanthan gum does adsorb on the rock surface despite its nonionic nature. Neutral guar gum shows the highest degree of adsorption when compared to the cationic guar and the gelling agent, due to its high polarity (shown in **Fig. 8**). The positive charge on the cationic guar polymer causes it to have a high degree of adsorption despite lower polarity. However, it is difficult to determine how much of that

non-ionicity has an impact on adsorption when compared with the molecular weight of the polymer without knowing the polymer's exact molecular weight.

4.5 Effect of Salinity on Polymer Adsorption

An attempt was made to further study this adsorption mechanism by introducing different brines to the polymer solution. The Marcellus shale was selected for this experiment, mainly because its clay content between is the Barnett (50%wt clays) and Eagle Ford (9.1%wt clays) shales at 25%wt (mostly illite).

The rheology of the polymer solutions with different brines was measured and is shown in **Fig. 19.** We can see that the viscosity of the polymer solution was reduced with the presence of each of the three brines. It is believed that the added brines would form a complex with the polymer molecules, shielding the ionic charges along the polymer chains. This causes the polymer to coil, which lessens the repulsive forces among the charges and results in a decrease in the hydrodynamic activity of the polymer in solution (Zhang et al., 2005).

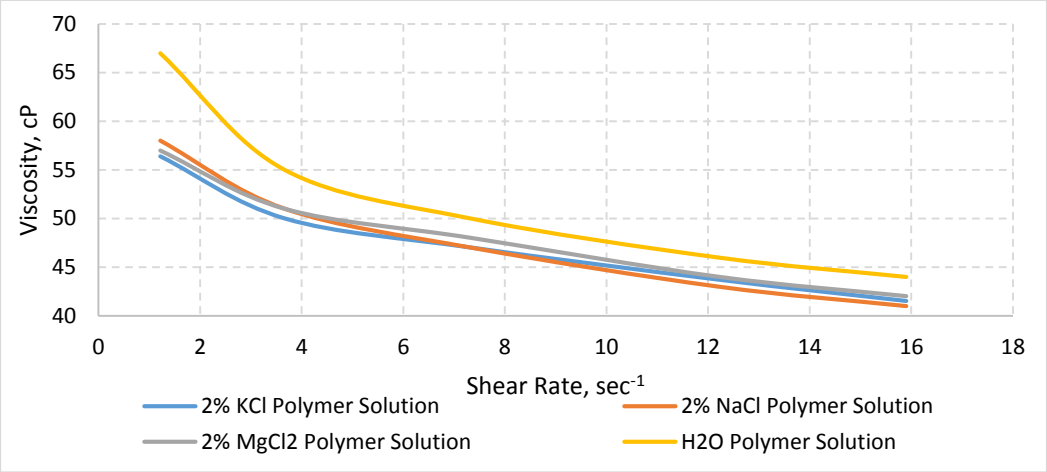

Fig. 19: Rheologies of different brine polymer solutions compared to water polymer solution

Shown in **Fig. 20** are viscosity reduction percentages for each polymer solution when exposed to Marcellus shale. Mg^{2+} is more hydrated than Na^{+} and K^{+} (Saini and MacLean, 1966) according to the Hofmeister Series. Additionally, the Marcellus shale is composed of 16% illite, which is highly water-wet. This could cause the free magnesium ions to adsorb on the surface of the rock, thus occupying the adsorption sites on the rock surface, previously saved for the polymer molecules. Therefore, there is a lesser viscosity reduction of the gelling agent polymer solution in the presence of 2% $MgCl_2$ as compared to 2% KCl and 2% NaCl gelling agent polymer solutions.

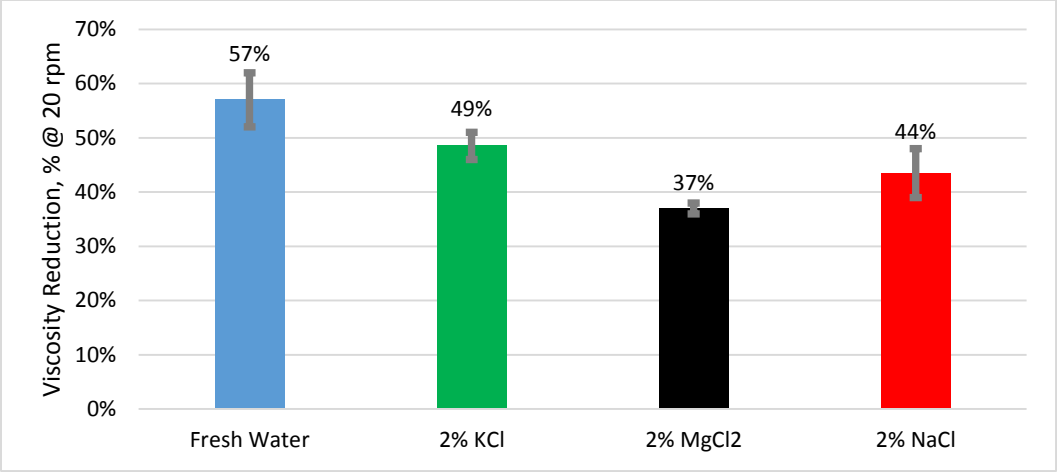

Fig. 20: Viscosity reduction in 2% KCl, NaCl, MgCl2, commercial gelling agent solutions compared to water gelling agent solution exposed to Marcellus samples for 24 hours at 115 °F. Shown are average values of three different experiments with standard error bar

Essentially, the above figure can be explained as two adsorption mechanisms occuring at the same time. The polymer molecules are adsorbed on the rock surface, with hydrogen bonding as the main adsorption mechanism in this case. Additionally, potassium, sodium, and magnesium ions are adsorbed on the water-illite (and to some extent, the other water-wet clay minerals). The more hydrated the ions are per Hofmeister's Series, the higher the degree of adsorption of these ions that can be expected. The end result is a competition between the polymer molecules and ions over adsorption sites on the surface of the rock. Furthermore, water soluble polymer molecules tend to uncoil less in solution with higher ionic strength of the solution. In such cases (in brines *vs.* fresh water), there is less polymer molecule available to bond to clay surface, leading to less strong bonding to that surface

and probably less total bonding of the polymer to the surface, which is consistent with observations that less polymer bonding to clay surfaces occurs in brines *vs.* fresh water.

4.6 Source Rock Interactions with Cross-Linked Borate Gel

Further examination of the interaction of source rocks with fracturing fluid was done using cross-linked fluids. The same procedure as the previous expertiments was followed as far as experimental set-up, with the only difference being a higher temperature (200 °F) to allow activation of the oxidizing gel breaker. **Fig. 21** shows the results from this work. The results are reported as actual values of viscosity rather than a reduction because the original viscosity of the borate cross-linked solution could not be measured.

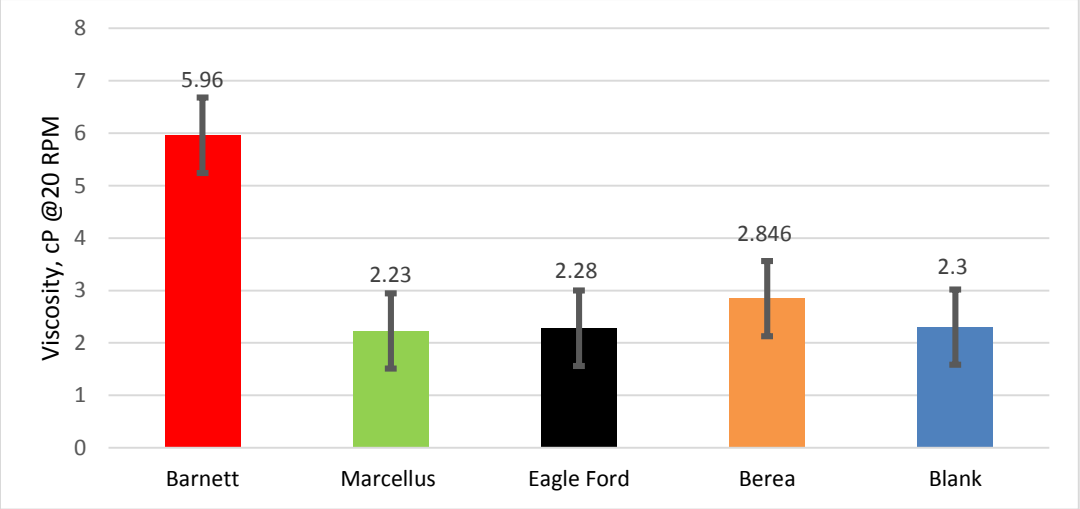

Fig. 21: Viscosity of the broken gel after exposing it to different rocks for 1 day at 200 °F. Shown are average values of three different experiments with standard error bars.

It is easy to observe that the viscosity of the broken gel for the Barnett shale case is higher than the rest of the cases. At this point, we were prompted to read study done by Anderson (1963) when sodium hypochlorite was used as an oxidizing agent to remove the organic content from soil samples. Sodium hypochlorite is used because of its powerful oxidizing capability, which functions in a similar manner to ammonium persulfate and sodium bromate. From this it was established that the gel breakers used in this experiment were possibly being spent on removing the organic content of the rock rather than being spent on breaking the cross-linked gel. This might significantly delay wellbore clean-up post fracture operation, which could severly impact cash-flow. Additionally, the presence of a viscous fluid inside the fracture indicates the presence of a high molecular weight polymer. This could in turn cross-link in the presence of borate ions and high pH (both of which are presumed to be present inside the fracture according to Agim (2014). If cross-linked gels are left unbroken for extended periods of time, they will keep cross-linking to a point where the gel would expel all the water out leaving a highly concentrated solid polymer concentrate inside the fracture. The latter could result in severe damage to the proppant pack conductivity (Marpaung et al. 2008).

The same procedure outlined in Anderson (1963) was followed to remove the organic content (described in Appendix A) from crushed Barnett Shale samples. Commercial bleach (6% sodium hypochlorite) was used. FTIR measurements were performed on the untreated and treated samples to determine if the method was successful in removing the organic content (**Fig. 22)**. We see the C-H stretch apparent disappearance at 2900 cm^{-1} for

the treated sample. The treated sample was then exposed to a cross-linked fluid under the same conditions (100 psi; 200 °F) and the viscosity of the broken gel was measured at 20 rpm (**Fig. 23**). The viscosity of the broken gel in the case of the treated sample was less than the untreated sample.

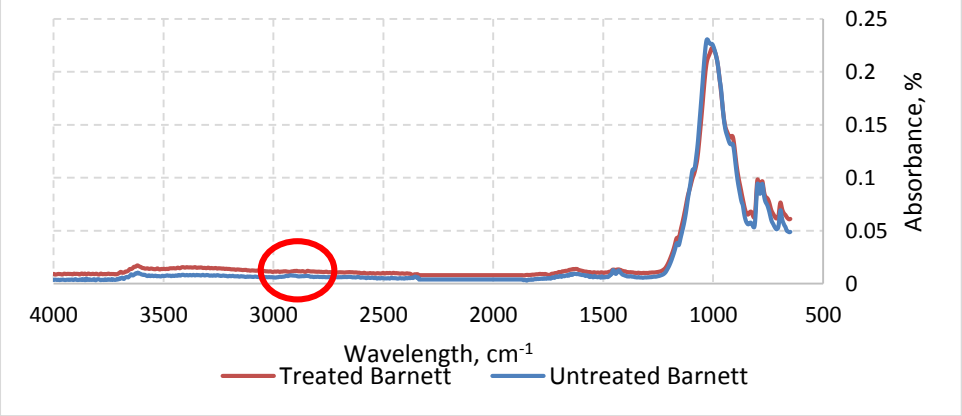

Fig. 22: Possible disappearance of C-H bond stretch (2900 cm-1) for treated Barnett sample

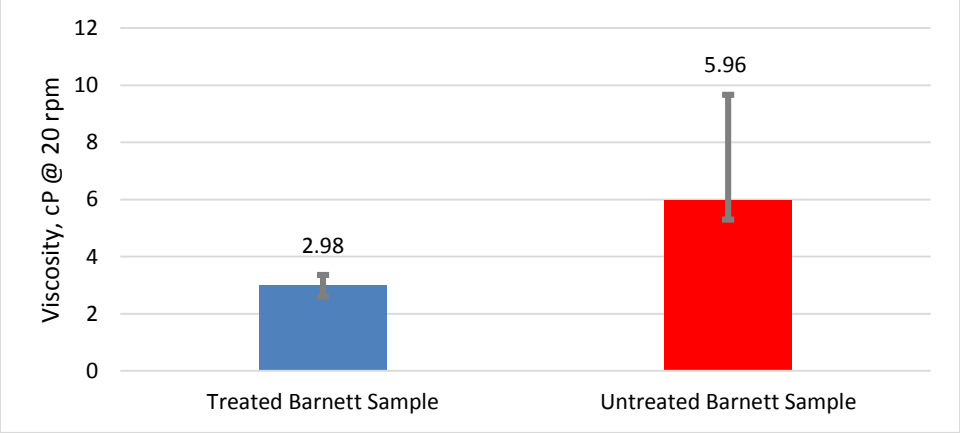

Fig. 23: Viscosity of the broken gel (made from commercial gelling agent) after exposing cross-linked fluid to treated and untreated Barnett samples for 24 hours under 200 °F. Shown are average values with standard error bars.

5. CONCLUSIONS AND RECOMMENDATIONS

The experiments done in this work revealed that there are significant molecular level interactions between the surface of the rock and the polymers studied. It is not yet understood how these interactions can affect the productivity of back-produced fracture fluid or the hydrocarbon- producing well. For example, viscosity reduction through polymer adsorption may be useful in aiding wellbore clean-up, after fracturing operations. Additionally, the study determined that one organic additive in fracturing fluids was possibly being lost to the rock through adsorption. This property could be used in reducing water treatment cost for reuse and disposal.

knowing that losing some of the organic material (polymers) to the rock can reduce water treatment cost for reuse and disposal. All these are beneficial uses of polymer adsorption. At the same time, polymer adsorption can potentially negatively impact well productivity by hampering inflow from the matrix to the fracture. Ueda and Harada's (1968) study has showed that the cation exchange capacity of the surface of the clays was being neutralized by polymer adsorption. This phenomenon could bring up the question of whether oilfield applications (i.e. use of surfactants) that depend on cation exchange capacity are affected by polymer adsorption.

- A workflow for the characterization of source rocks is presented here, which could help in the analysis of source rocks' interactions with water-based fluids. Other characterization methods might be developed in the future, which could reveal more detail and/or improve the analysis.

- It has been demonstrated here that there is a significant interaction between the rock samples and all the polymers used in this study.
- Viscosity reduction shown in this study was consistent with polymer adsorption, and correlates positively with the cation exchange capacity of the rock and its surface area.
- Thermal Degradation of the polymer could result in significant viscosity reduction of the polymer solution's viscosity in high temperature reservoirs.
- Dissolving polymer in 2% KCl, 2% NaCl, and 2% $MgCl_2$ solutions had varying impact on adsorption, with all reducing the amount of polymer adsorbed, and $MgCl_2$ having the highest impact.
- Polymer retention is impacted by the polymer's molecular weight, pH, the presence of divalent ions in the background solution, and the cation of cation exchange capacity of the rock.
- In some instances where the total organic content of some rocks is relatively high, the oxidizing gel breakers used might be spent on removing the organic content of the rock rather than being spent on breaking the cross-linked gel.
- Polymer adsorption could have some field ramifications; further study is needed to determine potential importance of such.

REFERENCES

Abdulsattar, Z. 2014. E-mail Communication from Yingqian Xiong. 7, XRD Sample Preparation.

Abdulsattar, Z., Agim, K., Lane, R. et al. 2015. Physico-Chemical Interactions of Source-Rocks with Injected Water-Based Fluids. Paper presented at the SPE International Symposium on Oilfield Chemistry, Woodlands, TX. USA. Society of Petroleum Engineers. SPE-173727-MS.

Aboulkas, A. and El Harfi, K. 2008. Study of the Kinetics and Mechanisms of Thermal Decomposition of Moroccan Tarfaya Oil Shale and Its Kerogen. *Oil Shale* **4** (25): 426-443.

Adhikary, P. and Singh, R.P. 2004. Synthesis, Characterization, and Flocculation Characteristics of Hydrolyzed and Unhydrolyzed Polyacrylamide Grafted Xanthan Gum. *Journal of Applied Polymer Science* **94** (1): 1411-1419.

Agim, K. 2014. Analysis of Water-Based Fracture Fluid Flowback to Determine Fluid/Shale Chemical Interaction. Master of Science, Texas A&M University, College Station, TX, USA.

Alramahi, B. and Sundberg, M.I. 2012. Proppant Embedment and Conductivity of Hydraulic Fractures in Shales. . Paper presented at the 46th U.S. Rock Mechanics/Geomechanics Symposium.

Anderson, J.U. 1963. An Improved Pretreatment for Mineralogical Analysis of Samples Containing Organic Matter *Clays and Clay Minerals* **10** (172): 380-388.

Avachat, A.M., Dash, R.R., and Shrotriya, S.N. 2011. Recent Investigations of Plant Based Natural Gums, Mucilages and Resins in Novel Drug Delivery Systems. *Indian Journal of Pharmaceutical Education and Research* **44** (1): 46-99.

Bailey, L., Keall, M., Audibert, A. et al. 1994. Effect of Clay/Polymer Interactions on Shale Stabilization During Drilling. *Langmuir* **10** (5): 1544-1549.

Belvalkar, R.A. and Oyewole, S. 2010. Development of Marcellus Shale in Pennsylvania. Paper presented at the SPE Annual Technical Conference and Exhibition, Florence, Italy. Society of Petroleum Engineers SPE-134852-MS.

Blauch, M.E. 2010. Developing Effective and Environmentally Suitable Fracturing Fluids Using Hydraulic Fracturing Flowback Waters. Paper presented at the SPE Unconventional Gas Conference, Pittsburgh, Pennsylvania, USA. Society of Petroleum Engineers SPE-131784-MS.

Bruner, K.A. and Smosna, R. 2011. *A Comparative Study of the Mississippian Barnett Shale, Fort Worth Basin, and Devonian Marcellus Shale, Appalachian Basin*. URS Corporation, San Francisco, CA.

Burger, J., Sourieau, P., and Combarnous, M. 1985. *Thermal Methods of Oil Recovery*. Imprimerie Nouvelle, France: Editions OPHRYS. Original edition.

Carroll, D. 1959. Ion Exchange in Clays and Other Minerals. *Geological Society of America Bulletin* **70** (6): 749-779.

Chapman, H.D. 1965. *Methods of Soil Analysis (Edited by Black, C. A.) Part 2*. Number 9 in the Series Agronomy. Madison, WI: American Institute of Agronomy. Original edition.

Chaudary, A.S. 2011. Shale Oil Production Performance from a Stimulated Reservoir Volume. Master of Science, Texas A&M University, College Station, TX, USA.

Cipolla, C.L., Lolon, E.P., Erdle, J.C. et al. 2010. Reservoir Modeling in Shale-Gas Reservoirs. *SPE Reservoir Evaluation & Engineering* **13** (04): 638-653.

Civan, F. 2007. Chapter 2 - Mineralogy and Mineral Sensitivity of Petroleum-Bearing Formations*. In *Reservoir Formation Damage (Second Edition)*, ed. Civan, F., Burlington: Gulf Professional Publishing.

Dealy, J.M. and Wang, J. 2013. Melt Rheology and Its Applications in the Plastics Industry. In *Springer Science+Business Media*, ed. Processes, E.M.a., Dordrecht.

Dohrmann, R. 2006. Cation Exchange Capacity Methodology Iii: Correct Exchangeable Calcium Determination of Calcareous Clays Using a New Silver–Thiourea Method. *Applied Clay Science* **34** (1–4): 47-57.

Easley, T.G., Sigal, R., and Rai, C. 2007. Thermogravimetric Analysis of Barnett Shale Samples. Paper presented at the International Symposium of the Society of Core Analysts, Calgary, Alberta, Canada. Society of Core Analysts.

Ewy, R.T. and Morton, E.K. 2009. Wellbore-Stability Performance of Water-Based Mud Additives. *SPE Drilling & Completion* **24** (3): 390-397.

Ewy, R.T. and Stankovic, R.J. 2010. Shale Swelling, Osmosis, and Acoustic Changes Measured under Simulated Downhole Conditions. *SPE Drilling & Completion* **25** (2): pp. 177-186.

Fontaine, J.S., Johnson, N.J., and Schoen, D. 2008. Design, Execution, and Evaluation of a "Typical" Marcellus Shale Slickwater Stimulation: A Case History. Paper presented at the SPE Eastern Regional/AAPG Eastern Section Joint Meeting, Pittsburgh, Pennsylvania, USA. Society of Petroleum Engineers SPE-117772-MS.

Frantz, J.H., Sawyer, W.K., MacDonald, R.J. et al. 2005. Evaluating Barnett Shale Production Performance Using an Integrated Approach. Paper presented at the SPE Annual Technical Conference and Exhibition, Dallas, Texas. Society of Petroleum Engineers SPE-96917-MS.

Gupta, A.P. and Arora, G. 2012. Preperation and Characterization of Cross-Linked Guar-Gum Poly(Vinylalcohol) Green Films *Der Chemica Sinica* **3** (5): 1191-1197.

Harris, W. and White, G. 2008. Methods of Soil Analysis Part 5—Mineralogical Methods. In *Soil Science Society of America Book Series*, ed. April L. Ulery, R.D., Madison, WI: Soil Science Society of America.

Hawkins, G.W. 1988. Laboratory Study of Proppant-Pack Permeability Reduction Caused by Fracturing Fluids Concentrated During Closure. Paper presented at the SPE Annual Technical Conference and Exhibition, Houston, Texas. Society of Petroleum Engineers.

Husain, T.M., Yeong, L.C., Saxena, A. et al. 2011. *Economic Comparison of Multi-Lateral Drilling over Horizontal Drilling for Marcellus Shale Field Development*. Pennsylvania State University.

Issarani, R. and Nagori, B.P. 2005. Effect of Gamma Radiation on Solution Viscosity of Galactomannans: Influence of Galactose : Mannose Ratio. *Indian Journal of Chemical Technology* **12** (1): 105-107.

Kale, S.V., Rai, C.S., and Sondergeld, C.H. 2010. Petrophysical Characterization of Barnett Shale. Paper presented at the SPE Unconventional Gas Conference, Pittsburgh, Pennsylvania, USA. Society of Petroleum Engineers SPE-131770-MS.

Kern, L.R. 1962. *Method and Composition for Formation Fracturing*, Office, U.P.

Khan, R., Kuru, E., Trembla, B. et al. 2003. An Investigation of Formation Damage Characteristics of Xanthan Gum Solutions Used for Drilling, Drill-in, Spacer Fluids, and Coiled Tubing Application. Paper presented at the Petroleum Society's Canadian International Petroleum Conference, Calgary, Alberta, Canada.

King, P.L., Ramsey, M.S., and Swayze, G.A. 2004. Infrared Spectroscopy in Geochemistry, Exploration Geochemistry, and Remote Sensing. In *Infrared Spectroscopy in Geochemistry, Exploration Geochemistry, and Remote Sensing*, ed. P.L.King, M.S.R., and G.A. Swayze, Canada. 33.

Kostenuk, N.H. and Browne, D.J. 2010. Improved Proppant Transport System for Slickwater Shale Fracturing. Paper presented at the Canadian Unconventional Resources and International Petroleum Conference, Calgary, Alberta, Canada. Society of Petroleum Engineers. SPE-137818-MS.

Leonard, R.S., Woodroof, R.A., Bullard, K. et al. 2007. Barnett Shale Completions: A Method for Assessing New Completion Strategies. Paper presented at the SPE Annual Technical Conference and Exhibition, Anaheim, California, U.S.A. Society of Petroleum Engineers SPE-110809-MS.

Letey, J. 1994. Adsorption and Desorption of Polymers on Soil. *Soil Science* **158** (4): 244-248.

Lowe, D.F., Oubre, C.L., and Ward, C.H. 1999. *Surfactants and Cosolvents for Napl Remediation a Technology Practices Manual*: CRC Press. Original edition.

Ma, X. and Pawlik, M. 2005. Effect of Alkali Metal Cations on Adsorption of Guar Gum onto Quartz. *Journal of Colloid and Interface Science* **289** (1): 48-55.

Manger, G.E. 1963. Porosity and Bulk Density of Sedimentary Rocks *Geological Survey Bulletin* **1** (114-E).

Marpaung, F., Chen, F., Pongthunya, P. et al. 2008. Measurement of Gel Cleanup in a Propped Fracture with Dynamic Fracture Conductivity Experiments. Paper presented at the SPE Annual Technical Conference and Exhibition, Denver, Colorado, USA. Society of Petroleum Engineers.

Merriman, R.J., Highley, D.E., and Cameron, D.G. 2003. *Definition and Characteristics of Very - Fine Grained Sedimentary Rocks: Clay, Mudstone, Shale, and Slate*. British Geological Survey.

Mody, F.K. and Hale, A.H. 1993. Borehole-Stability Model to Couple the Mechanics and Chemistry of Drilling-Fluid/Shale Interactions. *Journal of Petroleum Technology* **45** (11): 1093-1101.

Montgomery, C. 2010. Hydraulic Fracturing History of an Induring Technology. *Journal of Petroleum Technology* **12** (62): 26-32.

Montgomery, C. 2013. Fracturing Fluid Components. Paper presented at the International Conference for Effective and Sustainable Hydraulic Fracturing, Brisbane, Australia. International Society for Rock Mechanics. ISRM-ICHF-2013-034.

Montgomery, C. and Smith, M.B. 2010. Hydraulic Fracturing: History of an Enduring Technology. *Journal of Petroleum Technology* **62** (12): 26-32.

Mudgil, D., Barak, S., and Khatkar, B.S. 2012. X-Ray Diffraction, IR Spectroscopy and Thermal Characterization of Partially Hydrolyzed Guar Gum. *International Journal of Bioliological Macromolecules* **50** (4): 1035-1039.

Mullen, J. 2010. Petrophysical Characterization of the Eagle Ford Shale in South Texas. Paper presented at the Canadian Unconventional Resources and International Petroleum Conference, Calgary, Alberta, Canada. Society of Petroleum Engineers SPE-138145-MS.

Mullen, J., Lowry, J.C., and Nwabuoku, K.C. 2010. Lessons Learned Developing the Eagle Ford Shale. Paper presented at the Tight Gas Completions Conference, San Antonio, Texas, USA. Society of Petroleum Engineers SPE-138446-MS.

Palisch, T.T., Duenckel, R.J., Bazan, L.W. et al. 2007. Determining Realistic Fracture Conductivity and Understanding Its Impact on Well Performance - Theory and Field Examples. Paper presented at the SPE Hydraulic Fracturing Technology Conference, College Station, TX, USA. Society of Petroleum Engineers. SPE-106301-MS.

Palisch, T.T., Vincent, M., and Handren, P.J. 2010. Slickwater Fracturing: Food for Thought. *SPE Production & Operations* **25** (03): 327-344.

Parfitt, R.L. 1972. Adsorption of Charged Sugars by Montmorillonite. *Soil Science* **113** (6): 417-417.

Parfitt, R.L. and Greenland, D.J. 1970. The Adsorption of Polyethelyne Glycol on Clay Minerals. *Clay Minerals* **8** (1): 305-315.

Pawlik, M. and Laskowski, J.S. 2006. Stabilization of Mineral Suspensions by Guar Gum in Potash Ore Flotation Systems. *The Canadian Journal of Chemical Engineering* **84** (5): 532-538.

Penny, G.S., Dobkins, T.A., and Pursley, J.T. 2006. Field Study of Completion Fluids to Enhance Gas Production in the Barnett Shale. Paper presented at the SPE Gas Technology Symposium, Calgary, Alberta, Canada. Society of Petroleum Engineers. SPE-100434-MS.

Ping, Z.H., Nguyen, Q.T., Chen, S.M. et al. 2001. States of Water in Different Hydrophilic Polymers — Dsc and Ftir Studies. *Polymer* **42** (20): 8461-8467.

Prado, B.N.M., Kim, S., Zen, B.F.O. et al. 2005. Differentiation of Carbohydrate Gums and Mixtures Using Fourier Transform Infrared Spectroscopy and Chemometrics. *Journal of Agricultural and Food Chemistry* **53** (1): 2823-2829.

Ramurthy, M., Barree, R.D., Kundert, D.P. et al. 2011. Surface-Area Vs. Conductivity-Type Fracture Treatments in Shale Reservoirs. *SPE Production & Operations* **24** (04): 357-367.

Rassenfoss, S. 2011. From Flowback to Fracturing: Water Recycling Grows in the Marcellus Shale. *Journal of Petroleum Technology* **63** (7): 4.

Remvik, F. 1995. Shale-Fluid Interaction and Its Effect on Creep. Paper presented at the 8th ISRM Congress, Tokyo, Japan. International Society for Rock Mechanics. ISRM-8CONGRESS-1995-064

Ross, D.S. and Ketterings, Q. 2011. *Recommended Methods for Determining Soil Cation Exchange Capacity*. Recommended Soil Testing Procedures for the Northeastern United States. Newark, DE: Northeast Coordinating Committee for Soil Testing. Original edition.

Saini, G.R. and Maclean, A.A. 1966. Adsorption-Flocculation Reactions of Soil Polysaccharides with Kaolinite. *Soil science Society* **30** (1): 697-699.

Schamp, N. and Huylebroeck, J. 1973. Adsorption of Polymers on Clays. *Journal of Polymer Science: Polymer Symposia* **42** (2): 553-562.

Schloesing, T. 1874. Determination De L'argile Dans La Terre Arable. *Comptes rendus de l'Académie des Sciences* **78** (1): 1276-1279.

Speight, J. 1999. *The Chemistry and Technology of Petroleum*: CRC Press, 1999. New York, NY. Original edition.

Sun, H., Chawathe, A., Hoteit, H. et al. 2015. Understanding Shale Gas Flow Behavior Using Numerical Simulation. *SPE Journal* **20** (1): 142-154.

Theng, B.K.G. 1982. Clay-Polymer Interactions: Summary and Perspectives. *Clays and Clay Minerals* **30** (1): 1-10.

Tian, Y., Ayers, W., and McCain, W. 2013. The Eagle Ford Shale Play, South Texas: Regional Variations in Fluid Types, Hydrocarbon Production and Reservoir Properties. Paper presented at the 6th International Petroleum Technology Conference, Beijing, China. IPTC-16808-MS.

Tiraferri, A., Chen, K., Sethi, R. et al. 2008. Reduced Aggregation and Sedimentation of Zero-Valent Iron Nanoparticles in the Presence of Guar Gum. *Journal of Colloid and Interface Science* **324** (1–2): 71-79.

Ueda, T. and Harada, S. 1968. Adsorption of Cationic Polysulfone on Bentonite. *Journal of Applied Polymer Science* **12** (11): 2395-2401.

Ungewiß, J., Vietzke, L., Rapp, C. et al. 2005. Quantitative Determination of Cationic Modified Polysaccharides on Hair Using Lc–Ms and Lc–Ms–Ms. *Analytical Bioanalytical Chemistry* **381** (2005): 1401-1407.

Wang, J., Somasundaran, P., and Nagaraj, D.R. 2005. Adsorption Mechanism of Guar Gum at Solid–Liquid Interfaces. *Minerals Engineering* **18** (1): 77-81.

Weaver, J., Parker, M., van Batenburg, D. et al. 2007. Fracture-Related Diagenesis May Impact Conductivity. *SPE Journal* **12** (3): 272-281.

Weaver, J.D., Nguyen, P.D., Parker, M.A. et al. 2005. Sustaining Fracture Conductivity. Paper presented at the SPE European Formation Damage Conference, Sheveningen, The Netherlands. Society of Petroleum Engineers. SPE-94666-MS.

Whitcomb, P.J. and Macosko, C.W. 1978. Rheology of Xanthan Gum. *Journal of Rheology* **22**: 493-505.

Yang, Y., Robart, C., and Ruegamer, M. 2013. Analysis of U.S. Hydraulic Fracturing Design Trends. Paper presented at the 2013 SPE Hydraulic Fracturing Technology Conference, The Woodlands, TX, USA. Society of Petroleum Engineers. SPE-163875-MS.

Zhang, L., Zhou, J., and Hui, P. 2005. A Comparative Study on Viscosity Behavior of Water-Soluble Chemically Modified Guar Gum Derivatives with Different Functional Lateral Groups. *Journal of the Science of Food and Agriculture* **85** (15): 2638-2644.

APPENDIX

Sample preparation for XRD analysis (Abdulsattar, 2014)

1- The bulk samples are first pulverized to fine powder using a planetary ball mill with agate elements. Specimens for XRD analysis are front-loaded with a blade, with sieve rotation to ensure random grain orientation.

2- The clay fractions are separated in deionized water. Clay suspensions are then deposited by vacuum on 0.45-μm Whatman filters and transferred to glass slides.

3- Each concentrated clay sample are air-dried prior to XRD analysis and then saturated by ethylene glycol for subsequent analysis. Occasionally a heat treatment is necessary, in which case the slides are heated for 1 hour at 550 °C prior to further XRD analysis.

Procedure for Calculating Cation Exchange Capacity (CEC) (Chapman, 1965)

1. Pack approximately .5 g filter pulp into each sample tube.
2. Weigh 2.50 g < 2 mm air dry soil and transfer into sample tube. Install tubes in the upper disc of the extractor.
3. Install Na syringes.
4. Using a squeeze bottle containing pH 8.2 NaOAc, wash down the inside of the sample tubes.
5. Add NaOAc to the 20 ml mark of each sample tube.
6. Extract rapidly until the depth above each sample pad is about 3 to 5 ml.

7. Install Na reservoirs.
8. Add about 40 ml of NaOAc to each reservoir.
9. Extract for 2 hours; remove reservoirs.
10. Discard NaOAc extract.
11. Return extractor to starting position.
12. Reattach Na syringes to sample tubes.
13. Rinse wall of sample tube with ethanol and fill to 20 ml mark.
14. Extract rapidly until the depth of ethanol above each sample pad is 3 to 5 ml.
15. Install NH_4 reservoirs and fill to 40 ml mark with ethanol.
16. Extract for 45 min.
17. Remove reservoir and syringe and discard ethanol extracts.
18. Return extractor to starting position and add about 5 ml of ethanol to the sample. Reattach the NH_4 reservoirs.
19. Add about 40 ml of ethanol to NH_4 reservoirs and extract for 45 mins.
20. Remove reservoirs, discard ethanol, and return extractor to starting position.
21. Install numbered syringes.
22. Add pH 7.0 NH_4OAc to 20 ml mark.
23. Extract rapidly until depth of NH_4OAc above sample pad is about 3 to 5 ml.
24. Install NH_4 reservoirs and fill to 40 ml mark with NH_4OAc.
25. Extract for 2 hours.
26. Remove syringes. Transfer extract to a tared bottle and record weight of extract.

27. Determine concentration of Na in the extract by flame emisssion on the atomic absorption spectrometer. Use standards with the proper matrix (NH_4OAc) at 0, 5, 20, 40 ppm.
28. CEC is calculated using the following equation:

$$CEC\ \left(\frac{meq}{100g}\right) = (exract\ weight)\left(\frac{mg}{1Na}\right)(Dilution)(weight) * 230$$

Procedure for removing the organic content of the rock (modified from Anderson, 1963)

Oxidization:

1. Use 20 mL aliquot of sodium hypochlorite (bleach) freshly adjusted to a pH of 9.5 and add it to a beaker containing the cruched rock sample.
2. Place the beaker in a boiling water bath while stirring vigorously using a glass rod for 15 minutes.
3. Place the sample in two different centrifuge tubes and centrifuge them for 5 to 10 minutes at 800 rpm.
4. Decant the solution and repeat the treatment for a total of 3 times.

Washing:

1. add 50 mL aliquot of 2% sodium carbonate-sodium bicarbonate (15% $CaCO_3$-85% $NaHCO_3$) with a pH of 9.5 to the sample in a clean beaker.
2. place the beaker in a boiling water bath while stirring vigorously for 10-15 minutes to promote flocculation.

3. Place the sample in 2 different centrifuge tubes and centrifuge for 10 minutes at 800 rpm.
4. Decant the solution and repeat the treatment for a total of 3 times.
5. Dry the sample in an oven at 85 °C.